rabbits in physiological saline containing 2 mg/mL bovine serum albumin. Blood was collected from the opposite ear after injection at 5 min, 1 h, 2 h, 4 h, 6 h, and 28 h. ^{125}I-labeled apolipoprotein B-containing LDL was precipitated with 20% of trichloroacetic acid (Wako Pure Chemical Industries) (serum; 320 μL, 100% w/v trichloroacetic acid (TCA) 80 μL), and then the precipitants were applied for counting.

Uptake of DiO-labeled LDL by transplants ex vivo

Human LDL (1.019–1.063 g/mL) was isolated by sequential ultracentrifugation from normolipidemic donors as previously described,[24] dialyzed against saline-EDTA, and then sterilized by filtration through a 0.2 μm filter. Lipoproteins were labeled with 3,3'-dioctadecyloxacarbocyanine perchlorate (DiO; Sigma) by incubating the LDL in 0.5% bovine serum albumin/PBS with 100 mL DiO in dimethyl sulfoxide (3 mg/mL) for 8 h at 37°C. The lipoproteins were obtained by sequential ultra centrifugation (1.019–1.063 g/mL) as described,[14] and then dialyzed against PBS and filtered before use. To evaluate the uptake of DiO-LDL by transplants *ex vivo*, thin-sliced WHHL rabbit liver tissue were incubated with serum-free Dulbecco's modified Eagle's medium containing 10 μg/mL DiO-LDL for 24 h at 37°C. Finally, the incubated slices were rinsed, fixed with 10% formalin, sectioned into 5 μm thickness, and mounted with Perma-Flour (Japan Tanner Corporation). The slides were examined using a BioZero laser scanning microscope (Kyence).

Statistical analysis

Values were expressed as mean ± standard error of the mean. Differences between mean values of treated and untreated groups were evaluated using the Student's *t*-test. A p-value < 0.05 was considered statistically significant. All statistical analyses were performed using the SPSS Statistics 17.0 package (SPSS Inc.).

Results

Characteristics of hADMPCs

The cells obtained from adipose tissue were seeded and incubated for 24 h (Fig. 1Ai). After incubation, the adherent cells were treated with EDTA solution, and the resulting suspended cells were replated at a density of 10,000 cells/cm^2 on human fibronectin-coated dishes (BD BioCoat) (Fig. 1Aii and 1Aiii). Within two to three passages after the initial plating of the primary culture, hADMPCs appeared as a monolayer of large flat cells (25–30 μm in diameter). As the cells approached confluence, they assumed a more spindle-shaped, fibroblastic morphology (Fig. 1Aiv). After passaging five to six times, the hADMPCs were applied for transplantation. We used flow cytometry to assess markers expressed by hADMPCs (Fig. 1B). The cells were negative for markers of the hematopoietic lineage (CD45) and of hematopoietic stem cells, ABCG-2, CD34, and CD133. They were also negative for CD31, an endothelial cell-associated marker and the surface antigen c-Kit (CD117). However, they stained positively for a number of surface markers characteristic of mesenchymal and/or neural stem cells, but not embryonic stem cells, including CD29, CD44 (hyaluronan receptor), CD73, CD105 (endoglin), and CD166. hADMPCs also were positive for stage-specific embryonic antigen-4. Next, adipogenic, osteogenic, and chondrogenic differentiation potential of hADMPCs were examined (Fig. 1C). Adipogenic differentiation was induced by culture with differentiation medium containing 1-methyl-3-isobutylxanthine (a peroxisome proliferator-activated receptor γ agonist), dexamethasone, and insulin. Induction was confirmed by the accumulation of intracellular lipid droplets that were stained with Oil Red O. After 7-day induction for osteogenesis, hADMPCs were stained with Alizarin red S for mineralized nodules. hADMPCs showed intense Alcian Blue staining, indicating chondrogenic induction capability of hADMPCs.

Serum cholesterol in WHHL rabbit with transplants

hADMPCs were separated from human subcutaneous adipose tissues, cultured for five to seven passages, and applied for transplantation into WHHL rabbits. WHHL rabbits received immunosuppressants and an antiviral agent as illustrated in Figure 2A, and then were transplanted 3×10^7 hADMPCs by portal vein infusion (Fig. 2B). At the day of and 1, 2, 4, 6, and 10 weeks after transplantation of hADMPCs via the portal vein, we examined whether the cells reside or not in the liver after transplantation. Typical

FIG. 4. **(A)** Immunohistochemical identification of human hepatocytic marker cells in liver sections of WHHL rabbits after hADMPC transplantation. Twelve weeks after hADMPC transplantation, human albumin-, human alpha-1-antitrypsin-, human bile salt export pump (BSEP)-, and LDL-receptor-positive cells were dispersed within the perivenous regions of the liver parenchyma, where they made contact with and integrated among the host cells with cell–cell interactions between hADMPC-derived cells and diseased hepatocytes pair. Ten weeks after transplantation of DiI-stained hADMPCs, copresence of human albumin (green) and pretreated DiI-fluorescence (red) on the same cells was observed. Bar = 100 μm. **(B)** Differentiation of transplanted hADMPCs into hepatocyte-like cells. Twelve weeks after transplantation, almost but not all human CD90-positive cells expressed human albumin, indicating that major population of transplanted hADMPCs could differentiate into hepatocyte-like cells (left panel: human CD90; middle panel: human albumin; right panel: merge). Arrows indicate human CD90 and human albumin double-positive cells; arrowheads indicate human CD90-positive but human albumin-negative cells. **(C)** Human hepatic gene expression in WHHL rabbit liver after hADMPC transplantation. RNA was prepared from the WHHL rabbit liver 12 weeks after hADMPC transplantation. We used the following hepatic markers: human alpha-1-antitrypsin, human albumin, human factor IX, human GATA-binding protein 4 (GATA-4), human hepatocyte nuclear factor 3 (HNF-3) beta, and human LDL-receptor. Their expression levels were examined by quantitative real time-polymerase chain reaction (RT-PCR) using Assays-on-Demand Gene Expression Assay Mix. The livers of WHHL rabbits that received saline ($n = 3$) were negative for human hepatic genes. The mRNA levels were normalized based on human glyceraldehyde-3-phosphate dehydrogenase expression as housekeeping gene and data are mean ± SEM of triplicate experiments. The livers of WHHL rabbits that received hADMPC transplantation ($n = 3$) were positive for human hepatic genes, and their expression levels were similar to those of human primary hepatocytes but not hADMPCs *per se*. Data are mean ± SEM.

distribution patterns of transplanted hADMPCs were followed in Figure 2C. DiI-fluorescent labeled-hADMPCs resided and distributed in the portal area at the day of transplantation. Six and 10 weeks after transplantation, DiI-positive transplanted cells migrated into centrilobular direction. Next, to demonstrate certain percentage of repopulation of the transplanted cells in the liver, the ratios of human-derived cell repopulation were examined by analyzing a repetitive DNA sequence at the day of and 2, 4, 6, and 12 weeks after transplantation (Fig. 2D). To indicate standard curve, we mixed the indicated percentage of hADMPCs with rabbit hepatocytes and plotted the obtained the amount of *Alu* PCR products, and estimated the amount of repopulation of the transplanted cells in the liver. At the day of transplantation, the ratio of hADMPCs to whole WHHL rabbit liver cells was $0.21\% \pm 0.056\%$ (mean ± standard error of the mean) and the ratio decreased to $0.016\% \pm 0.002\%$, $0.011\% \pm 0.001\%$, and $0.009\% \pm 0.0001\%$ after 2, 4, and 8 weeks of transplantation, respectively. After 12 weeks of transplantation, the ratio was increased to $0.024\% \pm 0.00005\%$ as indicated (Fig. 2D).

To reveal the effects of hADMPC transplantation onto the lipid profiles of the WHHL rabbit, serum cholesterol levels were monitored over 12 weeks (Fig. 3A). Significant reductions in total serum cholesterol were observed within 4 weeks of the transplantation, and the reductions were maintained for the entire period. The reduction in serum cholesterol in the animals that received hADMPC transplantation was significantly greater than that of the control group. To determine the effects of hADMPC transplantation on the fractions of high-density lipoprotein and LDL in recipient animals, fractionation by fast protein liquid chromatography was performed (Fig. 3B). Transplantation of hADMPCs resulted in marked reduction of the peak LDL-cholesterol and increment of high-density lipoprotein cholesterol fraction (right panel).

Next, clearance experiments were performed with human LDL to confirm that the transplanted hADMPCs contributed the fall in serum cholesterol through uptake of LDL via LDL receptors. The rate of LDL clearance was significantly higher in the WHHL rabbits with transplanted hADMPCs than WHHL rabbits without transplanted hADMPCs (Fig. 3C). Rabbits with hADMPC transplants showed ~2.4-fold (high-dose; 3×10^7 cells/rabbit) and 1.4-fold (low-dose; 5×10^6 cells/rabbit) increase in the rate of LDL cholesterol clearance.

To evaluate the uptake of DiO-LDL by transplants *ex vivo*, thin-sliced WHHL rabbit liver was incubated with DiO-labeled LDL for 24 h and the uptake was examined as clearance experiment (Fig. 3D). DiO-LDL was uptaken by some but not all of the cells in the WHHL rabbit liver transplanted with hADMPCs. The DiO-LDL-uptaking cells were seen dispersed, contacted, and integrated among the nonuptaking parenchymal cells, suggesting that hADMPCs differentiated into hepatocytes *in vivo*, lowered of serum cholesterol via LDL uptake.

hADMPCs reside, survive, and differentiate into hepatocytes in vivo

After establishment of the graft as indicated by long-term lowering of serum cholesterol, human-specific hepatocytic proteins, such as albumin, alpha-1-antitrypsin, bile salt export pump, and LDL-receptor, positive cells were identified dispersed within perivenous regions of the liver parenchyma, where they have contacted and integrated among the host cells (Fig. 4A), with cell–cell interactions conserved between hADMPC-derived hepatocytes and diseased hepatocytes pair. Ten weeks after transplantation of DiI-prestained hADMPCs, copresence of human albumin (green) and pretreated DiI-fluorescence (red) on the same cells was observed (Fig. 4A), indicating the transplanted hADMPCs might differentiate into hepatocyte-like cells. To confirm transplanted hADMPCs might differentiate into hepatocyte-like cells and to reveal the efficacy of differentiation, the colocalization of human CD90 and human albumin was examined. As shown in Figure 4B, almost but not all human CD90-positive cells expressed human albumin, indicating that about 80% or more of transplanted hADMPCs could differentiated into human albumin-positive hepatocyte-like cells 12 weeks after transplantation. Next, to confirm the differentiation of hADMPCs into hepatocytes *in vivo*, expression of hepatocyte markers was analyzed by quantitative RT-PCR. The WHHL rabbit liver that was transplanted with hADMPCs expressed higher levels of human-specific alpha-1-antitrypsin, albumin, and coagulation factor IX than hADMPCs (Fig. 4C). The expression levels of human GATA-4, human hepatocyte nuclear factor 3 beta, and LDL-receptor were also higher in the WHHL rabbit liver than hADMPCs (Fig. 4C). These results indicate that hADMPCs differentiate into mature hepatocytes *in vivo*.

Discussion

We have used the WHHL rabbit to study the ability of hADMPC-derived hepatocytes to lower serum cholesterol in an animal model of FH. Our results have shown that hADMPCs transplanted into the rabbit liver differentiate into hepatocytes *in vivo* and effectively clear LDL from the circulation.

The reductions in cholesterol brought about by the engrafted hADMPC-derived hepatocytes suggest that human LDL receptors can act as replacement for the mutant LDL receptors in the WHHL rabbit. This capacity of hADMPC-derive hepatocytes is not unexpected, as the liver is the most important site of LDL uptake, accounting for >50% of total removal from the circulation, and the liver is only organ capable of converting cholesterol to bile for excretion. The substantial decrease in serum cholesterol achieved suggests that the hADMPC-derived hepatocytes both internalize LDL and metabolize the cholesterol to bile for excretion. The correlation between cholesterol and coronary heart disease has been well documented, and decreases in serum cholesterol of the magnitude that we have demonstrated would be expected to decrease morbidity and mortality in the patients with severe FH.[25]

The appearance of the hADMPC-derived hepatocytes as revealed by immunohistochemistry and RT-PCR indicated that the hADMPCs differentiated into hepatocytes and integrated into the liver parenchyma. The perivenous migration of the differentiated hepatocytes derived from hADMPCs along the portal-venous axis and suggests that hADMPCs recognize conserved signals on host cells and matrix. There are some reports describing the hepatogenic differentiation potential of hADMPCs.[15,16] These studies

described that hepatocytes differentiated from hADMPCs *ex vivo* engrafted in the liver and functioned, and that the hADMPCs could be resided and changed their characters into hepatocyte-like cells only in the chemically damaged liver. These reports, revealing that hADMPCs have capabilities to differentiate into hepatocytes, hinted us that hADMPCs might differentiate into hepatocytes in liver. Hepatogenic signals from the microenvironment such as cell-to-cell connections or intermediates are probably important factors that dictate the type of functional hepatocytes in hepatic differentiation.[26] We are currently investigating the mechanism for the differentiation hADMPCs into hepatocytes.

The choice of cell source is critical for realizing success in cellular therapy. Liposuction surgeries yield a massive amount of lipoaspirate adipose tissue from 100 mL to >3 L as cell sources.[27] A major advantage of hADMPCs is their availability in safe and easy with few ethical issues, as compared with the shortage of human livers for orthotopic transplantation, which has been shown to be effective for the treatment of FH.[25] Our serum cholesterol reduction studies and *in vitro* studies demonstrated that human LDL binds to the hADMPC-derived hepatocytes receptor, indicating that this therapy will be useful in humans. Previous attempts to study the efficacy of hepatocyte transplantation in the WHHL rabbit model have employed allogenic hepatocytes, xenogenic hepatocytes, or hepatocytes transduced *ex vivo* with a recombinant retrovirus containing the LDL receptor cDNA.[6–13] The lowering effects of hepatocyte transplantation on serum cholesterol have been reported, but there was some problems. First, hepatocytes could not be expanded *ex vivo* with functional potentials; second, the cell viability reduced after cryopreservation; third, the many injected hepatocytes are supposed to be cleared by the reticuloendothelial system or lose viability during early phase. The rate of LDL clearance was returned to normal in LDL receptor knockout mice by introduction of an adenoviral construct containing an LDL receptor cDNA, and similar approaches have lowered serum cholesterol levels in the WHHL rabbit.[10,12,13] However, sustained expression of the LDL receptor from viral vectors can be difficult to achieve.[11,13] Moreover, hepatocytes derived from hADMPCs have the advantage that the LDL receptor is expressed from an endogenous gene with intact regulatory sequences. Such control of LDL receptor levels would not be expected after treatment of hypercholesterolemia with LDL receptor cDNA construct that lack the regulatory regions of the gene.[28]

Our experiments have shown that the hADMPCs expressed hepatocyte markers after transplantation *in vivo* and the integrated cells into parenchyma provide functional LDL receptors, indicating that they differentiated into hepatocytes and might lower serum cholesterol in the WHHL rabbit. These results suggested that hADMPC transplantation via portal vein could correct the metabolic defects of FH patients and that hADMPC-derived hepatocytes could function as supplier with plasma proteins derived from liver, giving us an idea that hADMPC-transplantation might be a novel cell therapy for hemophilia, alpha-1 antitrypsin deficiency, mucolipidosis, and other diseases caused by genetic defects for liver function. In near future, the therapy will be a novel therapy for kinds of inherited liver diseases.

Acknowledgments

This study was supported in part by the Program for Promotion of Fundamental Studies in Health Sciences of the National Institute of Biomedical Innovation (NIBIO), RIKEN Program for Drug Discovery and Medical Technology Platforms, and Kobe Translational Research Cluster, the Knowledge Cluster Initiative, Ministry of Education, Culture, Sports, Science and Technology (MEXT).

Disclosure Statement

All of the authors stated no conflict of interest.

References

1. Brown, M.S., and Goldstein, J.L. A receptor-mediated pathway for cholesterol homeostasis. Science **232,** 34, 1986.
2. Havel, R.J., Yamada, N., and Shames, D.M. Watanabe heritable hyperlipidemic rabbit. Animal model for familial hypercholesterolemia. Arteriosclerosis **9(I Suppl),** I33, 1989.
3. Yamamoto, T., Bishop, R.W., Brown, M.S., Goldstein, J.L., and Russell, D.W. Deletion in cysteine-rich region of LDL receptor impedes transport to cell surface in WHHL rabbit. Science **32,** 1230, 1986.
4. Bujo, H., Takahashi, K., Saito, Y., Maruyama, T., Yamashita, S., Matsuzawa, Y., Ishibashi, S., Shionoiri, F., Yamada, N., and Kita, T. Clinical features of familial hypercholesterolemia in Japan in a database from 1996–1998 by the research committee of the ministry of health, labour and welfare of Japan. J Atheroscler Thromb **11,** 146, 2004.
5. Yamashita, S., Hbujo, H., Arai, H., Harada-Shiba, M., Matsui, S., Fukushima, M., Saito, Y., Kita, T., and Matsuzawa, Y. Long-term probucol treatment prevents secondary cardiovascular events: a cohort study of patients with heterozygous familial hypercholesterolemia in Japan. J Atheroscler Thromb **15,** 292, 2008.
6. Gunsalus, J.R., Brady, D.A., Coulter, S.M., Gray, B.M., and Edge, A.S. Reduction of serum cholesterol in Watanabe rabbits by xenogeneic hepatocellular transplantation. Nat Med **3,** 48, 1997.
7. Tejera, M.L., Cienfuegos, J.A., Maganto, P., Pardo, F., Santamaria, L., Codesal, J., De Andres, S., Hernandez, J.L., and Castillo-Olivares, J.L. Reduction of cholesterol levels following liver cell grafting in hyperlipidemic (WHHL) rabbits. Transplant Proc **24,** 160, 1992.
8. Wang, J., Pollak, R., and Bartholomew, A. Sustained reduction of serum cholesterol levels following allo-transplantation of parenchymal hepatocytes in Watanabe rabbits. Transplant Proc **23,** 894, 1991.
9. Wiederkehr, J.C., Kondos, G.T., and Pollak, R. Hepatocyte transplantation for the low-density lipoprotein receptor-deficient state. A study in the Watanabe rabbit. Transplantation **50,** 466, 1990.
10. Chowdhury, J.R., Grossman, M., Gupta, S., Chowdhury, N.R., Baker, J.R., Jr., and Wilson, J.M. Long-term improvement of hypercholesterolemia after *ex vivo* gene therapy in LDLR-deficient rabbits. Science **254,** 1802, 1991.
11. Ishibashi, S., Brown, M.S., Goldstein, J.L., Gerard, R.D., Hammer, R.E., and Herz, J. Hypercholesterolemia in low density lipoprotein receptor knockout mice and its reversal by adenovirus-mediated gene delivery. J Clin Invest **92,** 883, 1993.
12. Kozarsky, K.F., McKinley, D.R., Austin, L.L., Raper, S.E., Stratford-Perricaudet, L.D., and Wilson, J.M. *In vivo* correction

of low density lipoprotein receptor deficiency in the Watanabe heritable hyperlipidemic rabbit with recombinant adenoviruses. J Biol Chem **269,** 13695, 1994.
13. Wilson, J.M., Chowdhury, N.R., Grossman, M., Wajsman, R., Epstein, A., Mulligan, R.C., and Chowdhury, J.R. Temporary amelioration of hyperlipidemia in low density lipoprotein receptor-deficient rabbits transplanted with genetically modified hepatocytes. Proc Natl Acad Sci U S A **87,** 8437, 1990.
14. Okura, H., Komoda, H., Saga, A., Kakuta-Yamamoto, A., Hamada, Y., Fumimoto, Y., Lee, C.M., Ichinose, A., Sawa, Y., and Matsuyama, A. Properties of hepatocyte-like cell clusters from human adipose tissue-derived mesenchymal stem cells. Tissue Eng Part C Methods **16,** 761, 2010.
15. Banas, A., Teratani, T., Yamamoto, Y., Tokuhara, M., Takeshita, F., Quinn, G., Okochi, H., and Ochiya, T. Adipose tissue-derived mesenchymal stem cells as a source of human hepatocytes. Hepatology **46,** 219, 2007.
16. Seo, M.J., Suh, S.Y., Bae, Y.C., and Jung, J.S. Differentiation of human adipose stromal cells into hepatic lineage *in vitro* and *in vivo*. Biochem Biophys Res Commun **328,** 258, 2005.
17. Komoda, H., Okura, H., Lee, C.M., Sougawa, N., Iwayama, T., Hashikawa, T., Saga, A., Yamamoto, A., Ichinose, A., Murakami, S., Sawa, Y., and Matsuyama, A. Reduction of N-glycolylneuraminic acid xenoantigen on human adipose tissue-derived stromal cells/mesenchymal stem cells leads to safer and more useful cell sources for various stem cell therapies. Tissue Eng Part A **16,** 1143, 2010.
18. Okura, H., Matsuyama, A., Lee, C.M., Saga, A., Kakuta-Yamamoto, A., Nagao, A., Sougawa, N., Sekiya, N., Takekita, K., Shudo, Y., Miyagawa, S., Komoda, H., Okano, T., and Sawa, Y. Cardiomyoblast-like cells differentiated from human adipose tissue-derived mesenchymal stem cells improve left ventricular dysfunction and survival in a rat myocardial infarction model. Tissue Eng Part C Methods **16,** 417, 2010.
19. Bjorntorp, P., Karlsson, M., Pertoft, H., Pettersson, P., Sjostrom, L., and Smith, U. Isolation and characterization of cells from rat adipose tissue developing into adipocytes. J Lipid Res **19,** 316, 1978.
20. Zuk, P.A., Zhu, M., Ashjian, P., De Ugarte, D.A., Huang, J.I., Mizuno, H., Alfonso, Z.C., Fraser, J.K., Benhaim, P., and Hedrick, M.H. Human adipose tissue is a source of multipotent stem cells. Mol Biol Cell **13,** 4279, 2002.
21. Nicklas, J.A., and Buel, E. Development of an Alu-based, real-time PCR method for quantitation of human DNA in forensic samples. J Forensic Sci **48,** 936, 2003.
22. Opel, K.L., Fleishaker, E.L., Nicklas, J.A., Buel, E., and McCord, B.R. Evaluation and quantification of nuclear DNA from human telogen hairs. J Forensic Sci **53,** 853, 2008.
23. Okazaki, M., Usui, S., Ishigami, M., Sakai, N., Nakamura, T., Matsuzawa, Y., and Yamashita, S. Identification of unique lipoprotein subclasses for visceral obesity by component analysis of cholesterol profile in high-performance liquid chromatography. Arterioscler Thromb Vasc Biol **25,** 578, 2005.
24. Bier, D.M., and Havel, R.J. Activation of lipoprotein lipase by lipoprotein fractions of human serum. J Lipid Res **11,** 565, 1970.
25. Steinberg, D., and Witztum, J.L. Current concepts. Lipoproteins and atherogenesis. Current concepts. JAMA **264,** 3047, 1990.
26. Hughes, R.D., Mitry, R.R., and Dhawan, A. Hepatocyte transplantation for metabolic liver disease: UK experience. J R Soc Med **98,** 341, 2005.
27. Gimble, J.M., Katz, A.J., and Bunnell, B.A. Adipose-derived stem cells for regenerative medicine. Circ Res **100,** 1249, 2007.
28. Bilheimer, D.W., Goldstein, J.L., Grundy, S.M., Starzl, T.E., and Brown, M.S. Liver transplantation to provide low-density-lipoprotein receptors and lower plasma cholesterol in a child with homozygous familial hypercholesterolemia. N Engl J Med **311,** 1658, 1984.

Address correspondence to:
Akifumi Matsuyama, M.D., Ph.D.
Department of Somatic Stem Cell Therapy and Health Policy
Foundation for Biomedical Research and Innovation
TRI305, 1-5-4 Minatojima-minamimachi, Chuo-ku
Kobe 650-0047
Japan

E-mail: akifumi-matsuyama@umin.ac.jp

Received: March 7, 2010
Accepted: August 9, 2010
Online Publication Date: September 21, 2010

Clinical Effectiveness of Boron Neutron Capture Therapy for a Recurrent Malignant Peripheral Nerve Sheath Tumor in the Mediastinum

Masayoshi Inoue, MD, PhD, Chun Man Lee, MD, PhD,† Koji Ono, MD, PhD,‡ Minoru Suzuki, MD, PhD,‡ Toshiteru Tokunaga, MD,* Yoshiki Sawa, MD, PhD,† and Meinoshin Okumura, MD, PhD**

A 70-year-old woman underwent extirpation of a malignant peripheral nerve sheath tumor, 4.5 × 2.0 cm in size, in the right supraclavicular fossa. Locoregional recurrence was found 10 months after operation (Figure 1). Although one course of systemic chemotherapy using cisplatin (80 mg/m^2 at day 1) and vinorelbine (25 mg/m^2 at days 1 and 8) was given, the recurrent tumor progressed. Because conventional radiotherapy is not effective for malignant peripheral nerve sheath tumor, boron neutron capture therapy (BNCT) was considered based on the subcutaneous mediastinal location. After institutional review board approval and securing the patient's written informed consent, accumulation of p-boronophenylalanine (BPA) in the tumor was confirmed using 18F-BPA positron emission tomography. Using simulation environment for radiation applications software program, fast neutron and γ-ray physical doses, compound biologic effectiveness- and relative biologic effectiveness-weighted doses, were calculated.

The patient underwent two courses of BNCT with an interval of 3 weeks. BPA-fructose was administered intravenously at a dose of 500 mg/kg just before irradiation. For the first course, the epithermal neutron irradiation was performed for 105 minutes. The dose distribution in the tumor ranged from 13.7 to 22.3 Gy-Eq and was 6.0 Gy-Eq to the skin. For the second course, the irradiation time was shortened to 51 minutes, because of the higher epithermal neutron flux. The dose delivered to the tumor ranged from 6.0 to 24.3 Gy-Eq and was 9.7 Gy-Eq to the skin.

Chest computed tomography scan 1 year after BNCT showed that the tumor size decreased from 6.2 × 4.0 cm to 4.6 × 3.2 cm in size (25% reduction), and stable disease was maintained for 24 months (Figure 2). Positron emission tomography-computed tomography 18 months after BNCT showed no uptake of 18F-fluorodeoxy glucose in the residual mass, suggesting no viability (Figure 3). Neuralgia of the right arm improved. Although temporary dysphagia because of an oral mucosa disorder was observed as a side effect, the patient's general quality of life was preserved. There is no evidence of recurrence 2 years after BNCT.

DISCUSSION

When ^{10}Boron absorbs thermal neutrons, α and ^{7}Lithium particles are generated.[1] BNCT selectively injures the tumor cells containing ^{10}Boron; it was suitable in this case with tumor invasion into the neighboring great vessels. Because the peak of thermal neutron flux is 3 cm beneath the tissue surface, its clinical applications have been limited to malignant melanomas and brain tumors. Kato et al.[2] reported its efficacy for head and neck malignancies. The indication was extended to metastatic liver tumor,[3] malignant mesothelioma,[4] and glioblastoma.[5] This is the first case of mediastinal tumor treated with BNCT.

The effect of BNCT is critically dependent on selective accumulation of ^{10}Boron compounds. The tumor/normal tissue ratio of the ^{10}Boron uptake was 2 in this case, while a ratio greater than 2.5 is preferable for selective treatment. BNCT might be a treatment option for subcutaneous mediastinal tumors, which is resistant to conventional irradiation.

REFERENCES

1. Barth RF, Coderre JA, Vicente MG, et al. Boron neutron capture therapy of cancer: current status and future prospects. *Clin Cancer Res* 2005; 11:3987–4002.
2. Kato I, Ono K, Sakurai Y, et al. Effectiveness of BNCT for recurrent head and neck malignancies. *Appl Radiat Isot* 2004;61:1069–1073.
3. Wittig A, Malago M, Collette L, et al. Uptake of two 10B-compounds in liver metastases of colorectal adenocarcinoma for extracorporeal irradiation with boron neutron capture therapy (EORTC Trial 11001). *Int J Cancer* 2008;122:1164–1171.
4. Suzuki M, Sakurai Y, Masunaga S, et al. Feasibility of boron neutron capture therapy (BNCT) for malignant pleural mesothelioma from a viewpoint of dose distribution analysis. *Int J Radiat Oncol Biol Phys* 2006;66:1584–1589.
5. Vos MJ, Turowski B, Zanella FE, et al. Radiologic findings in patients treated with boron neutron capture therapy for glioblastoma multiforme within EORTC trial 11961. *Int J Radiat Oncol Biol Phys* 2005;61:392–399.

*Department of General Thoracic Surgery, Osaka University Graduate School of Medicine, Suita, Osaka; †Medical Center for Translational Research, Osaka University Hospital, Suita, Osaka; and ‡Radiation Oncology Research Laboratory, Research Reactor Institute, Kyoto University, Kyoto, Japan.

Disclosure: The authors declare no conflicts of interest.

Address for correspondence: Meinoshin Okumura, MD, Department of General Thoracic Surgery, Osaka University Graduate School of Medicine, L5-2-2 Yamadaoka, Suita, Osaka 565-0781, Japan. E-mail: meinosin@thoracic.med.osaka-u.ac.jp

ISSN: 1556-0864/10/0512-2037

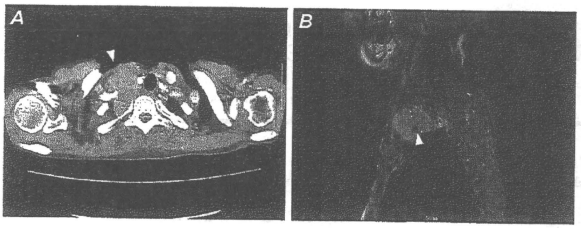

FIGURE 1. Chest computed tomography (CT) scan and magnetic resonance imaging (MRI) showing the recurrent lesion. *A*, Postoperative recurrence, 4.5 × 2.0 cm in size, is seen in the right subclavicular region (arrow head) in the follow-up CT scan 10 months after operation. *B*, Tumor invasion into the right subclavicular artery and brachiocephalic vein is seen (arrow head) in the sagittal view of MRI.

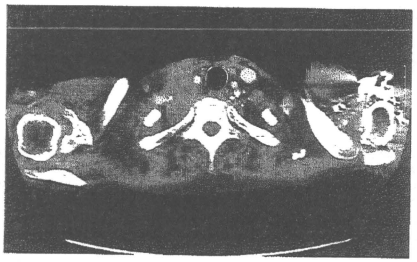

FIGURE 2. Chest computed tomography scan 1 year after boron neutron capture therapy shows shrinkage of the recurrent lesion after chemotherapy from 6.2 × 4.0 cm to 4.6 × 3.2 cm in size (25% reduction).

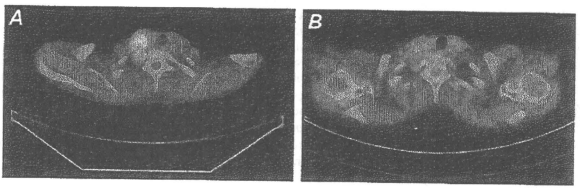

FIGURE 3. FDG-positron emission tomography (PET) shows the remarkable effect of boron neutron capture therapy (BNCT). *A*, PET-computed tomography (CT) before BNCT shows significant tumor uptake. *B*, Although a residual mass is seen, the FDG uptake is reduced to the background level 18 months after BNCT.

Mutation Research 695 (2010) 69–74

Contents lists available at ScienceDirect

Mutation Research/Genetic Toxicology and Environmental Mutagenesis

journal homepage: www.elsevier.com/locate/gentox
Community address: www.elsevier.com/locate/mutres

Ascorbic acid 2-glucocide reduces micronucleus induction in distant splenic T lymphocytes following head irradiation

Yuko Kinashi*, Hiroki Tanaka, Shinichiro Masunaga, Minoru Suzuki, Genro Kashino, Liu Yong, Sentaro Takahashi, Koji Ono

Research Reactor Institute, Kyoto University, Kumatori-cho, Sennan-gun, Osaka 590-0494, Japan

ARTICLE INFO

Article history:
Received 13 April 2009
Received in revised form 2 November 2009
Accepted 6 December 2009
Available online 16 December 2009

Keywords:
Abscopal radiation effect
Ascorbic acid
T lymphocyte
Micronucleus

ABSTRACT

Purpose: Evidence from in vivo studies suggests there are enhanced radiation effects in abscopal regions after local head gamma ray irradiation. Splenocyte apoptosis and T lymphocyte micronuclei were induced at higher rates than what would be estimated given the dose at a shielded, distant position. In addition, we evaluated the radio-protective effects of ascorbic acid, acting as a radical scavenger on enhanced radiation effects in the shielded spleen following local head irradiation.

Methods and materials: The heads of C3H mice were exposed to γ-rays (10–20 Gy), while the other parts of the body were shielded with a 5 cm-thick lead block. The effective dose for the spleen was calculated at 1.0–2.0 Gy. Splenocytes were isolated 24 h after cranial irradiation and their apoptosis was measured with an Elisa kit (Roche). The induction of T lymphocyte micronuclei was studied using the cytokinesis-block micronucleus assay. The ascorbic acid glucoside, 2-O-alpha-D-glucopyranosyl-L-ascorbic acid (AA-2G), was orally administered to mice 1 h before whole body irradiation. The radio protective effects of AA-2G were estimated by comparing the induction of splenocyte damage (by apoptosis) and micronucleus induction.

Results: The splenocyte damage, as measured by the above two methods, was more excessive than what would be expected given exposure to 1.0–2.0 Gy of radiation. Our results suggest that the effects were enhanced in a distant, non-irradiated organ after localized irradiation. Plasma ascorbic acid concentrations were increased 8–10× over control. Treatment with ascorbic acid slightly protected mouse splenocytes from the induction of apoptosis by the enhanced effects of radiation in the abscopal region. However, ascorbic acid significantly inhibited micronucleus induction in splenic T lymphocytes following local head irradiation.

Conclusions: Our results suggest that ascorbic acid effectively scavenged radiation-induced radicals and protected against the enhanced effects of radiation in an abscopal region after local head gamma ray irradiation.

1. Introduction

The abscopal effects of radiation were first reported in 1969 and were defined as significant responses to radiation in tissues that are separate from the area exposed to the radiation [1,2].

The enhanced effects of radiation in shielded organs are thought to be based on the phenomena of so-called bystander effects. Their mechanism is thought to involve radiation signals that are transduced from the radiation-targeted organ to shielded organs [3,4]. Most have been observed in the low-dose range [3,5,6]. In fact, Prise et al. [6] noted that most bystander effects appear to saturate at higher dose levels, and that other factors must switch to hypersensitivity of a non-targeted response.

Abscopal effects from radiation have also been previously reported at therapeutic doses. For example, in studies with partially irradiated lungs, animals and patients were reported to have higher than expected tissue damage in unirradiated parts of the lung [7,8]. The mechanism for this hypersensitivity of non-targeted responses has not been elucidated, but inflammatory responses and reactive oxygen species, such as superoxide radicals, are involved [2,9].

We previously published that bystander effects were observed after boron neutron capture therapy (BNCT), and found that the radical scavenger ascorbate could effectively protect from distant damage [10]. Another group reported that radical scavengers were protective against radiation-induced bystander effects in an in vitro study [11]. Here, we investigated the possibility that 2-O-alpha-D-glucopyranosyl-L-ascorbic acid (AA-2G) had clinically relevant

* Corresponding author. Tel.: +81 72 451 2437; fax: +81 72 451 2627.
E-mail address: kinashi@rri.kyoto-u.ac.jp (Y. Kinashi).

1383-5718/$ – see front matter © 2009 Elsevier B.V. All rights reserved.
doi:10.1016/j.mrgentox.2009.12.002

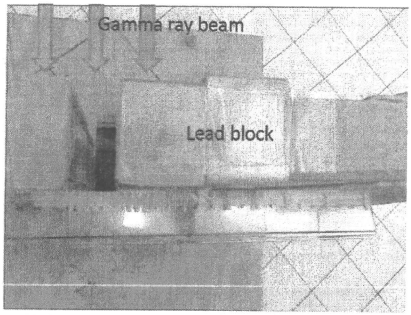

Fig. 1. A view from above showing the strategy for local head irradiation. The head of a mouse was irradiated while being held in a restrainer through a 2 cm slit, while the rest of its body was located behind a 5 cm lead block.

radio-protective effects. Its radio-protective effects were evaluated after induction of apoptosis in mouse splenocytes and micronuclei in splenic T cells, at a site that was distant from local head irradiation.

2. Materials and methods

2.1. Mice and ascorbic acid administration

Six-week-old female C3H/He mice were obtained from Japan Animal Inc. and acclimated to our laboratory for 8–10 weeks prior to use in experiments. AA-2G was purchased from Hayashibara Biochemical Laboratories (Okayama, Japan). C3H female mice (14–16 weeks old) were given AA-2G orally (dissolved in water, 1 mg/g of body weight), 1 h before gamma-ray irradiation. The concentration of AA-2G administration was decided after referencing previous experiments [12–14] and considering the high plasma accumulation and toxicity of ascorbic acid. Note: 1 mg of AA-2G is the equivalent of 0.52 mg of ascorbic acid. The ascorbic acid concentration in mouse plasma after AA-2G administration was measured by HPLC.

2.2. Irradiation

Gamma rays were delivered with a ^{60}Co gamma-ray machine at a rate of 1.0 Gy/min. Mice were restrained in a plastic box on a radiation shelf. For partial head irradiation, heads were placed in a 2.0 cm slit in the front side of the restrainer and the rest of their bodies were shielded behind a 5 cm-thick lead block (Fig. 1). The absorbed doses for the head and the body are shown in Fig. 2. For total body irradiation (to evaluate direct splenic damage following irradiation), the whole body was irradiated (up to 5 Gy).

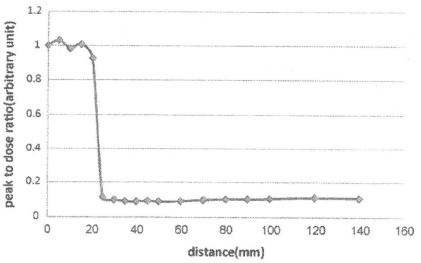

Fig. 2. Estimation of the amount of radiation passing through the 2 cm slit (the irradiated head dose) and into the area shielded by the lead block (the spleen dose). Each point corresponds to a red mark on the scale in Fig. 1. The intervals between the points were 5 mm (0–5 cm), 1 cm (5–10 cm) and 2 cm (10–14 cm). The head of the mouse was located in the first 2 cm (in the open region). The spleen was located at 4 cm. The dose given to the spleen was estimated at 1 Gy when 10 Gy of irradiation was given to the head.

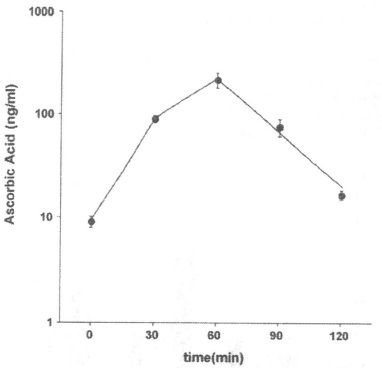

Fig. 3. The concentration of ascorbic acid in mouse plasma after AA-2G administration.

2.3. Isolation of splenocytes and splenic T lymphocytes

Details of the T lymphocyte isolation have been described elsewhere [15]. Briefly, after gamma irradiation, mice were sacrificed by cervical dislocation, and their spleens were removed, minced and washed twice in Hanks' balanced salt solution. Lymphocytes were separated using Ficoll-Hypaque gradients and were resuspended in RPMI 1640 medium (GIBCO) containing 10% fetal calf serum. The T lymphocytes were cultured at 37 °C in a humidified 5% CO_2 incubator. Optimum concentrations of Concanavalin A (Con A, 2 μg/mL) and 2-mercaptoethanol (2-ME, 50 μmol/mL) were used to make lymphocytes transform and divide in culture.

2.4. Radiation induced apoptosis and antioxidant enzyme activation

To determine splenocyte apoptosis, mice were sacrificed 24 h after irradiation and their spleens were removed. Single-cell suspensions were eliminated of erythrocytes by incubating at room temperature for 3 min in a solution of Tris-

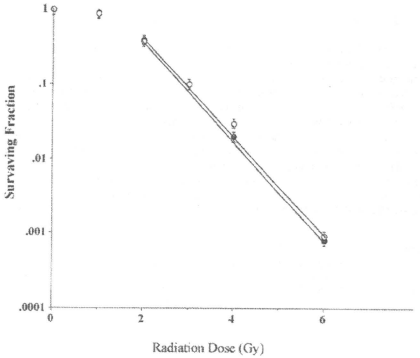

Fig. 4. Survival curves for splenic T lymphocytes following gamma irradiation with (open circle) or without (closed circle) ascorbic acid administration. Data represent the means ± SE of three different independent experiments. The curves for doses greater than 2 Gy were fit by linear regression analysis.

Table 1
Survival parameters for T lymphocytes after gamma ray irradiation with V.C. (ascorbic acid) treatment.

Treatment	D_0	D_{10}
Gamma ray radiation	0.65 ± 0.2 Gy	3.0 ± 0.2 Gy
Gamma ray radiation with V.C. treatment	0.85 ± 0.3 Gy	3.1 ± 0.2 Gy

Data pooled from three or more experiments; mean ± SE. D_0 and D_{10} derived from survival curves following irradiation.

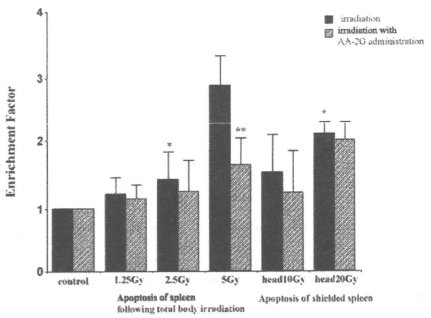

Fig. 5. Induction of apoptosis of mouse splenocytes after irradiation (black bars) and the effect of AA-2G administration (gray bars). Histogram bars show the means ± SE for five animals. (*) Significant increase in apoptosis compared to 2.5 Gy total body irradiation. $p < 0.05$. (**) Significant decrease in apoptosis compared to no ascorbic acid administration. $p < 0.05$.

buffered ammonium chloride. After twice washing with PBS, cells were counted and examined for induction of apoptosis. Apoptosis was detected with a sandwich immunoassay system using a cell death detection ELISA kit (Roche Diagnostic Inc.). The assay is based on the quantitative sandwich enzyme immunoassay principle, using mouse monoclonal antibodies directed against DNA and histones, respectively. Apoptosis was measured by following the ELISA protocol. The enrichment factor was the calculated absorbance of each sample divided by the absorbance of corresponding negative control. To measure the activity of catalase (CAT) and superoxide dismutase (SOD), mouse blood was obtained from the main inferior vein 60, 120 and 1200 min after irradiation. The activities of CAT and SOD in mouse plasma were detected using a colorimetric assay (SRL Research Laboratory Inc., Japan).

2.5. Determination of T lymphocyte survival and the micronucleus assay

Details of the assays for cell survival and micronucleus frequency have been reported previously [15]. Briefly, the survival data for lymphocytes were obtained by limiting dilution assays. To measure the cloning efficiency of lymphocytes, cells were seeded in culture medium (150 μL) at densities of 10–10,000 cells/well in 96-well tissue culture plates. The cloning efficiency was calculated from the proportion of the wells without clones, using limiting dilution analysis [16]. The cytokinesis-block micronucleus assay for lymphocytes was performed following a method described by Fenech and Morley [17] with slight modifications. Cytochalasin B (Sigma) was added to the cultured T lymphocytes at a final concentration of 5.0 μg/mL, 44 h after Con A stimulation. Eighteen hours later, cells were collected by centrifugation and resuspended in Carnoy's fixative. Next, a drop of the cell suspension was spread on a glass slide and dried, the cells were stained with Hoechst 33258 (50 μg/mL), and

Table 3
The micronucleus frequency per 100 binucleated T lymphocytes after irradiation and the effect of AA-2G administration.

Total body irradiation (Gy)			Head irradiation 10 Gy
0 Gy	1.25 Gy	2.5 Gy	
2.8 ± 1.5	26.8 ± 6.5	47.9 ± 13.2	62.1 ± 18.5
With AA-2G treatment			
2.9 ± 1.5	14.9 ± 8.5**	29.1 ± 11.5**	24.9 ± 10.5**

Results show the mean ± SE from at least three independent experiments.
** Significant differences were observed with AA-2G administration (Student's *t*-test; $p < 0.05$).

the frequency of micronuclei was determined on 10 separate slides by counting the total number of micronuclei per 100 binucleated cells.

2.6. Statistical analysis

Significance was calculated using Student's tests. Results were considered significant for values of $p < 0.05$.

3. Results

3.1. The effect of ascorbic acid treatment

The ascorbic acid concentration in mouse plasma increased and was maintained at a high level during the 30–90 min after oral administration of AA-2G. One hour after AA-2G administration (1 mg/g of mouse body weight), the concentration of ascorbic acid in the plasma was increased 4–10× over the control (Fig. 3). The plasma level of ascorbic acid increased sharply, as quickly as 30 min, and was maintained at a high level for 1.5 h after oral administration of AA-2G. The availability of AA-2G as ascorbic acid was compatible with a previous report [13].

Fig. 4 and Table 1 show survival curves and the parameters for T lymphocytes after gamma irradiation, with and without ascorbic acid treatment. These results showed that gamma radiation lethality was not affected by ascorbic acid treatment.

3.2. Induction of apoptosis and the activities of anti-oxidative enzymes

Apoptosis was analyzed after 1.25, 2.5 and 5 Gy of whole body irradiation and 10 and 20 Gy of local head irradiation, with and without ascorbic administration. For local head irradiation, the spleen was shielded behind a 5 cm-thick lead block (Fig. 1) and the doses of radiation absorbed by the spleen and head were measured (1.0 Gy for the spleen from 10 Gy of radiation exposure to the head; 2.0 Gy (spleen) from 20 Gy (head); Fig. 2). After 20 Gy head irradiation, the apoptosis that occurred in shielded spleen cells exceeded that which occurred when spleen cells were directly irradiated with 2.5 Gy (Fig. 5). Therefore, the damage to shielded spleen cells was more excessive than what would be expected given a dose of 2.0 Gy.

Fig. 5 also shows the induction of apoptosis in mouse splenocytes after AA-2G treatment. Ascorbic acid protected mouse

Table 2
SOD and catalase activity in mouse serum after treatment with AA-2G.

Time after irradiation (min)	SOD activity (Units/mL)		Catalase activity (Units/mL)	
	6 Gy irradiation	6 Gy irradiation with AA-2G	6 Gy irradiation	6 Gy irradiation with AA-2G
0	7.7 ± 0.8	7.1 ± 0.7	1.0 ± 0.1	1.0 ± 0.1
60	9.2 ± 0.9	10.4 ± 1.0	3.6 ± 0.4	4.2 ± 0.4
120	10.0 ± 0.9	11.0 ± 1.0	3.6 ± 0.4	4.4 ± 0.4
1200	12.5 ± 1.0	14.0 ± 1.4	2.2 ± 0.2	4.4 ± 0.4**

Results show the mean ± SE from at least three independent experiments.
** Significant increases were observed with AA-2G administration (Student's *t*-test; $p < 0.05$).

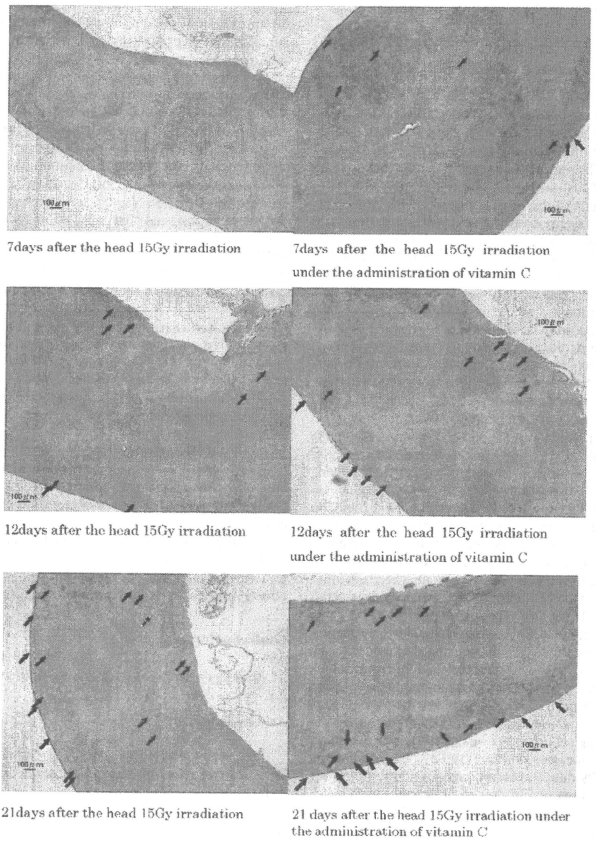

Fig. 6. Spleens 7–21 days after 15 Gy of head irradiation. Formalin-fixed paraffin-embedded tissue sections were HE stained. The arrows show macrophage proliferation in the spleen after the head irradiation (magnification 30×. Scale bars 100 μm).

splenocytes from apoptosis after 5 Gy whole-body irradiation. To understand how anti-oxidative enzymes participate in initial DNA damage, we investigated how treating with AA-2G affected the activation of the CAT and SOD in the plasma following a dose of 6 Gy (1 Gy in addition to the 5 Gy irradiation). AA-2G administration increased the activation of CAT and SOD slightly. A significant increase in CAT activity was observed with AA-2G treatment 20 h after irradiation (Table 2).

3.3. Micronucleus induction

The induction of micronuclei in mouse T lymphocytes after various treatments is shown in Table 3. Micronuclei were counted after 1.25 and 2.5 Gy of whole body irradiation and 10 Gy of local head irradiation, with and without ascorbic administration. As mentioned above, a 10 Gy dose of radiation exposure to the head corresponded to a dose of 1.0 Gy for the shielded spleen. The frequency of micronuclei induced in shielded splenic T cells with 10 Gy of head irradiation was about 2 times higher than that induced after 2.5 Gy of whole body irradiation (Table 3). Our results confirm that shielded, distant splenic T lymphocytes had more damage than what would have been anticipated, given a dose of 1.0 Gy. This again suggests that the radiation effects in a distant, shielded organ were enhanced after local irradiation. However, while treatment with ascorbic acid protected, although not significantly, against the induction of apoptosis in shielded splenocytes, ascorbic acid significantly inhibited shielded splenic T lymphocytes from forming micronuclei after local head irradiation (Fig. 5 and Table 3). Therefore, unlike its effects on induction of mouse splenocyte apoptosis, AA-2G had radioprotective

effects on the induction of T lymphocyte micronuclei after irradiation.

4. Discussion

In high LET therapy, as occurs in boron neutron capture therapy (BNCT) and heavy-ion radiotherapy, hypo-fractionation is acceptable and therapeutic radiation doses are larger than conventional radiotherapies. The normal tissue radiation dose for vascular endothelial cells in BNCT is estimated to be around 10–15 Gy [18]. Enhanced radiation effects in abscopal regions following large local doses of radiation have not previously been investigated. Here, we studied whether shielded splenocytes in abscopal regions suffered enhanced radiation effects after 10–20 Gy of local head gamma ray-irradiation. Splenocyte apoptosis induction and T lymphocyte micronuclei were higher than what would be expected with the estimated dose of radiation in the distant, shielded spleen.

In vivo radiation-induced bystander effects are defined as phenomena that occur when irradiation signals are transduced from an irradiated lesion to a shielded organ and induce a radiation effect in that non-irradiated, shielded organ. A previous group reported that the spleen is a target organ of local-irradiation induced bystander effects in vivo. Koturbash et al. described how cranial X-ray irradiation (1 Gy) induced DNA damage, apoptosis, and increased p53 levels in a shielded spleen [5]. They also suggested the possibility that the induction of indirect DNA damage in the shielded splenocytes was mediated by reactive oxygen species. Mechanistically, the radiation-induced bystander effect in vivo is thought to be mediated by the inflammatory response after exposure to ionizing radiation. Lorimore et al. reported that macrophage activation following a 4 Gy irradiation provided a mechanism for producing damage via bystander effects [19]. Another previous report showed that tumor cell killing by macrophages was activated with more than 10 Gy [20]. These experiments show that high dose radiation might induce bystander signaling by mediating macrophage activation. We confirmed that large dose local head irradiation (10–20 Gy) induced apoptosis and micronuclei in the distant, shielded spleen. These enhanced radiation effects in an abscopal region were induced by a large dose irradiation and may have been mediated by macrophage activation. Shown in the left column of Fig. 6, histological sections revealed macrophage proliferation in the spleen appearing on the 12th day post-irradiation and becoming severe by day 21. Macrophage proliferation in the spleen was found to be more severe after ascorbic acid administration, and to occur earlier (on the 7th day post-irradiation; shown in the right column of Fig. 6).

We evaluated the protective effects of a radical scavenger on enhanced radiation effects in the distant spleen after large doses of local head irradiation. Free radicals are one of the most important bio-chemicals that are triggered by the activation of macrophages following irradiation [21]. This suggests the possibility that radical scavengers might protect abscopal regions from enhanced radiation effects. Our study of apoptosis induction suggests that AA-2G treatment suppressed the induction of apoptosis following total body radiation. In our anti-oxidative enzyme study, AA-2G administration increased catalase activity after 20 h, which was the length of the apoptosis assay, but AA-2G did not significantly affect SOD activity. The C3H/He mouse strain is more radiation-resistant than other Balb/c mouse strains [22,23]. The different sensitivities of mouse strains to irradiation were determined by micronucleus formation in T lymphocytes and fibroblasts, and an intestinal cell survival assay [15]. A previous report demonstrated that hepatic CAT and SOD enzyme activities increased 30 min after whole body ionizing irradiation of C3H mice, suggesting that CAT and SOD may be related to the mechanism of their radiation resistance [24]. We confirmed that these antioxidant enzymes had elevated activities after irradiation and that AA-2G enhanced CAT activity. This result suggests that ascorbic acid may protect from radiation damage by inducing CAT.

We previously reported that radical scavengers are protective against neutron-induced mutations [25,26]. Furthermore, we compared the effects of DMSO (a source of short-lived radical scavengers) and ascorbic acid (a source of long-lived radical scavengers) on the induction of mutations in bystander cells. DMSO treatment slightly reduced the frequency of mutations that were induced by the bystander effect, but post-radiation ascorbic-acid treatment reduced the mutation frequency more than DMSO [10]. Recently, Harada et al. reported that ascorbic acid was an effective radical scavenger for suppressing the bystander response in vitro. They examined three types of radical scavengers, including a nitric oxide scavenger, and found that ascorbic acid was the most effective suppressor of micronucleus induction in non-irradiated bystander cells [27].

We showed that ascorbic acid significantly inhibited shielded splenic T lymphocytes from forming micronuclei following local head irradiation (Fig. 5 and Table 3). However, AA-2G did not protect shielded splenocytes against apoptosis. These results show that AA-2G treatment had radio-protective effects on T-lymphocytes in abscopal regions (in the spleen), but this did not apply to all splenic cells.

Clinically, chromosomal instability [28] and epigenetic dysregulation of DNA [29] were analyzed in non-irradiated or distant organs after irradiation. Enhanced radiation effects in abscopal regions are thought to increase the incidence of secondary, post-radiation therapy cancers. Therefore, effective radioprotection from enhanced radiation effects in abscopal regions is needed. Ascorbic acid is a well-known, important vitamin and a non-toxic radical scavenger that can be effective for protecting against enhanced radiation effects in abscopal regions during radiation therapy.

Conflict of interest

Authors declare that there are no conflicts of interest.

Acknowledgments

This study was supported by a Grant-in-Aid for Scientific Research from the Ministry of Education, Culture, Sports, Science and Technology of Japan.

References

[1] M.P. Nobler, The abscopal effect in malignant lymphoma and its relationship to lymphocyte circulation, Radiology 93 (1969) 410–412.
[2] W.F. Morgan, Non-targeted and delayed effects of exposure to ionizing radiation: II. Radiation-induced genomic instability and bystander effects in vivo, clastogenic factors and transgenerational effects, Radiat. Res. 159 (2003) 581–596.
[3] K. Camphausen, M.A. Moses, C. Menard, M. Sproull, W.D. Beecken, J. Folkman, M.S. O'Reilly, Radiation abscopal antitumor effect is mediated through p53, Cancer Res. 63 (2003) 1990–1993.
[4] E.I. Azzam, J.B. Little, The radiation-induced bystander effect: evidence and significance, Hum. Exp. Toxicol. 23 (2004) 61–65.
[5] I. Koturbash, J. Loree, K. Kutanzi, C. Koganow, I. Pogribny, O. Kovalchuk, In vivo bystander effect: cranial X-irradiation leads to elevated DNA damage, altered cellular proliferation and apoptosis, and increased p53 levels in shielded spleen, Int. J. Radiat. Oncol. Biol. Phys. 70 (2007) 554–562.
[6] K.M. Prise, M. Folkard, B.D. Michael, A review of the bystander effect and its implications for low-dose exposure, Radiat. Protect. Dosimetry 104 (2003) 347–355.
[7] G.W. Morgan, S.N. Breit, Radiation and the lung: a re-evaluation of the mechanism mediating pulmonary injury, Int. J. Radiat. Oncol. Biol. Phys. 31 (1995) 361–369.
[8] M.A. Khan, R.P. Hill, J. Van Dyk, Partial volume rat lung irradiation: an evaluation of early DNA damage, Int. J. Radiat. Oncol. Biol. Phys. 40 (1998) 467–476.

[9] K.M. Prise, M. Folkard, B.D. Michael, Bystander response induced by low LET radiation, Oncogene 22 (2003) 7043–7049.
[10] Y. Kinashi, S. Masunaga, K. Nagata, M. Suzuki, S. Takahashi, K. Ono, A bystander effect observed in boron neutron capture therapy: a study of the induction of mutations in the HPRT locus, Int. J. Radiat. Oncol. Biol. Phys. 68 (2007) 508–514.
[11] G. Kashino, K.M. Prise, K. Suzuki, N. Matsuda, S. Kodama, M. Suzuki, K. Nagata, Y. Kinashi, S. Masunaga, K. Ono, M. Watanabe, Effective suppression of bystander effects by DMSO treatment of irradiated CHO cells, J. Radiat. Res. 48 (2007) 197–204.
[12] I. Yamamoto, S. Suga, Y. Mitoh, M. Tanaka, N. Muto, Antiscorbutic activity of L-ascorbic acid 2-gluciside and its availability as a vitamin C supplement in normal rats and guinea pigs, J. Pharmacobiodyn. 13 (1990) 688–695.
[13] A. Tai, Y. Fujitani, K. Matsumoto, D. Kawasaki, I. Yamamoto, Bioability of a series of novel acylated ascorbic acid derivatives, 6-O-acyl-2-O-α-D-glucopyranosyl-L-ascorbic acids, as an ascorbic acid supplement in rats and guinea pigs, Biosci. Biotechnol. Biochem. 66 (2002) 1628–1634.
[14] L.V. d'Uscio, S. Milstien, D. Richardson, L. Smith, Z.S. Katusic, Long-term Vitamin C treatment increase vascular tetrahydrobiopterin levels and nitric oxide synthase activity, Circulat. Res. 92 (2003) 88–95.
[15] Y. Kinashi, K. Ono, M. Abe, The micronucleus assay of lymphocytes is a useful predictive assay of the radiosensitivity of normal tissue: a study of three inbred strains of mice, Radiat. Res. 148 (1997) 341–347.
[16] H. Waldmann, S. Cobbold, I. Lefkovits, Limiting dilution analysis, in: G.G.B. Klaus (Ed.), Lymphocytes, A Practical Approach, IRL, Oxford, 1987, pp. 163–188.
[17] F. Fenech, A.A. Morley, Cytokinesis-block micronucleus method in human lymphocytes: effect of in vivo aging and low dose X-irradiation, Mutat. Res. 161 (1986) 193–198.
[18] T. Kageji, S. Nagahiro, S. Uyama, Y. Mizobuchi, Y. Nakagawa, Clinical review of BNCT using mixed neutron beam in patients with malignant glioma, in: W. Sauerwein, R. Moss, A. Wittig (Eds.), Research and Development in Neutron Capture Therapy Monduzzi Editore S.p.A., Bologna, Italy, 2002, pp. 1085–1091.
[19] S.A. Lorimore, P.J. Coates, G.E. Scobie, G. Milne, E.G. Wright, Inflammatory-type responses after exposure to ionizing radiation in vivo: a mechanism for radiation-induced bystander effects? Oncogene 20 (2001) 7085–7095.
[20] L.E. Lambert, D.M. Paulnock, Modulation of macrophage function by γ-irradiation: Acquisition of the primed cell intermediate stage of macrophage tumoricidal action pathway, J. Immunol. 139 (1987) 2834–2841.
[21] G. McLennan, L.W. Oberley, A.P. Author, The role of oxygen-derived free radicals in radiation-induced damage and death of nondividing eukaryotic cells, Radiat. Res. 84 (1980) 122–132.
[22] K.H. Kohn, M.M. Kallman, The influence of strain on acute X-ray lethality in the mouse: LD50 and death rate studies, Radiat. Res. 5 (1956) 309–317.
[23] T.H. Roderic, The response of twenty-seven inbred strains of mice to daily doses of whole-body X-irradiation, Radiat. Res. 120 (1963) 631–639.
[24] R. Hardmeier, H. Hoeger, S. Fang-Kircher, A. Khoschsorur, G. Lubic, Transcription and activity of antioxidant enzymes after ionizing irradiation in radiation-resistant and radiation-sensitive mice, Proc. Natl. Acad. Sci. U.S.A. 94 (1997) 7572–7576.
[25] Y. Kinashi, Y. Sakurai, S. Masunaga, M. Suzuki, M. Akaboshi, K. Ono, Dimethyl sulfoxide protects against thermal and epithermal neutron-induced cell death and mutagenesis of Chinese hamster ovary (CHO) cells, Int. J. Radiat. Oncol. Biol. Phys. 47 (2000) 1371–1378.
[26] Y. Kinashi, Y. Sakurai, S. Masunaga, M. Suzuki, K. Nagata, K. Ono, Ascorbic acid reduced mutagenicity at the HPRT locus in CHO cells against thermal neutron radiation, Appl. Radiat. Isotopes 61 (2004) 929–932.
[27] T. Harada, G. Kashino, K. Suzuki, N. Matsuda, S. Kodama, M. Watanabe, Different involvement of radical species in irradiated and bystander cells, Int. J. Radiat. Biol. 84 (2008) 809–814.
[28] E. Gwyneth, S.A. Watson, A. Lorimore, D.A. Macdonald, E.G. Wright, Chromosomal instability in unirradiated cells induced in vivo by a bystander effect of ionizing radiation, Cancer Res. 60 (2000) 5608–5611.
[29] I. Koturbash, A. Boyko, R. Rodriguez-Juarez, R.J. MacDonald, V.P. Tryndyak, I. Kovalchuk, I.P. Pogribny, O. Kovalchuk, Role of epigenetic effects in maintenance of long-term persistent bystander effect in spleen in vivo, Carcinogenesis 28 (2007) 1831–1838.

Mutation Research 695 (2010) 69–74

Contents lists available at ScienceDirect

Mutation Research/Genetic Toxicology and Environmental Mutagenesis

journal homepage: www.elsevier.com/locate/gentox
Community address: www.elsevier.com/locate/mutres

Ascorbic acid 2-glucocide reduces micronucleus induction in distant splenic T lymphocytes following head irradiation

Yuko Kinashi*, Hiroki Tanaka, Shinichiro Masunaga, Minoru Suzuki, Genro Kashino, Liu Yong, Sentaro Takahashi, Koji Ono

Research Reactor Institute, Kyoto University, Kumatori-cho, Sennan-gun, Osaka 590-0494, Japan

ARTICLE INFO

Article history:
Received 13 April 2009
Received in revised form 2 November 2009
Accepted 6 December 2009
Available online 16 December 2009

Keywords:
Abscopal radiation effect
Ascorbic acid
T lymphocyte
Micronucleus

ABSTRACT

Purpose: Evidence from in vivo studies suggests there are enhanced radiation effects in abscopal regions after local head gamma ray irradiation. Splenocyte apoptosis and T lymphocyte micronuclei were induced at higher rates than what would be estimated given the dose at a shielded, distant position. In addition, we evaluated the radio-protective effects of ascorbic acid, acting as a radical scavenger on enhanced radiation effects in the shielded spleen following local head irradiation.
Methods and materials: The heads of C3H mice were exposed to γ-rays (10–20 Gy), while the other parts of the body were shielded with a 5 cm-thick lead block. The effective dose for the spleen was calculated at 1.0–2.0 Gy. Splenocytes were isolated 24 h after cranial irradiation and their apoptosis was measured with an Elisa kit (Roche). The induction of T lymphocyte micronuclei was studied using the cytokinesis-block micronucleus assay. The ascorbic acid glucoside, 2-O-alpha-D-glucopyranosyl-L-ascorbic acid (AA-2G), was orally administered to mice 1 h before whole body irradiation. The radio protective effects of AA-2G were estimated by comparing the induction of splenocyte damage (by apoptosis) and micronucleus induction.
Results: The splenocyte damage, as measured by the above two methods, was more excessive than what would be expected given exposure to 1.0–2.0 Gy of radiation. Our results suggest that the effects were enhanced in a distant, non-irradiated organ after localized irradiation. Plasma ascorbic acid concentrations were increased 8–10× over control. Treatment with ascorbic acid slightly protected mouse splenocytes from the induction of apoptosis by the enhanced effects of radiation in the abscopal region. However, ascorbic acid significantly inhibited micronucleus induction in splenic T lymphocytes following local head irradiation.
Conclusions: Our results suggest that ascorbic acid effectively scavenged radiation-induced radicals and protected against the enhanced effects of radiation in an abscopal region after local head gamma ray irradiation.

1. Introduction

The abscopal effects of radiation were first reported in 1969 and were defined as significant responses to radiation in tissues that are separate from the area exposed to the radiation [1,2].

The enhanced effects of radiation in shielded organs are thought to be based on the phenomena of so-called bystander effects. Their mechanism is thought to involve radiation signals that are transduced from the radiation-targeted organ to shielded organs [3,4]. Most have been observed in the low-dose range [3,5,6]. In fact, Prise et al. [6] noted that most bystander effects appear to saturate at higher dose levels, and that other factors must switch to hypersensitivity of a non-targeted response.

Abscopal effects from radiation have also been previously reported at therapeutic doses. For example, in studies with partially irradiated lungs, animals and patients were reported to have higher than expected tissue damage in unirradiated parts of the lung [7,8]. The mechanism for this hypersensitivity of non-targeted responses has not been elucidated, but inflammatory responses and reactive oxygen species, such as superoxide radicals, are involved [2,9].

We previously published that bystander effects were observed after boron neutron capture therapy (BNCT), and found that the radical scavenger ascorbate could effectively protect from distant damage [10]. Another group reported that radical scavengers were protective against radiation-induced bystander effects in an in vitro study [11]. Here, we investigated the possibility that 2-O-alpha-D-glucopyranosyl-L-ascorbic acid (AA-2G) had clinically relevant

* Corresponding author. Tel.: +81 72 451 2437; fax: +81 72 451 2627.
E-mail address: kinashi@rri.kyoto-u.ac.jp (Y. Kinashi).

1383-5718/$ – see front matter © 2009 Elsevier B.V. All rights reserved.
doi:10.1016/j.mrgentox.2009.12.002

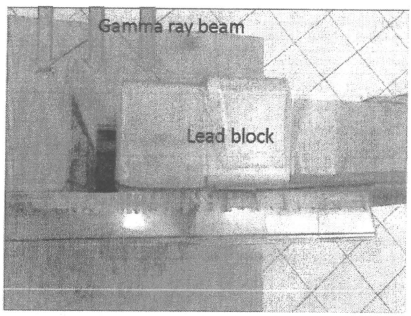

Fig. 1. A view from above showing the strategy for local head irradiation. The head of a mouse was irradiated while being held in a restrainer through a 2 cm slit, while the rest of its body was located behind a 5 cm lead block.

radio-protective effects. Its radio-protective effects were evaluated after induction of apoptosis in mouse splenocytes and micronuclei in splenic T cells, at a site that was distant from local head irradiation.

2. Materials and methods

2.1. Mice and ascorbic acid administration

Six-week-old female C3H/He mice were obtained from Japan Animal Inc. and acclimated to our laboratory for 8–10 weeks prior to use in experiments. AA-2G was purchased from Hayashibara Biochemical Laboratories (Okayama, Japan). C3H female mice (14–16 weeks old) were given AA-2G orally (dissolved in water, 1 mg/g of body weight), 1 h before gamma-ray irradiation. The concentration of AA-2G administration was decided after referencing previous experiments [12–14] and considering the high plasma accumulation and toxicity of ascorbic acid. Note: 1 mg of AA-2G is the equivalent of 0.52 mg of ascorbic acid. The ascorbic acid concentration in mouse plasma after AA-2G administration was measured by HPLC.

2.2. Irradiation

Gamma rays were delivered with a ^{60}Co gamma-ray machine at a rate of 1.0 Gy/min. Mice were restrained in a plastic box on a radiation shelf. For partial head irradiation, heads were placed in a 2.0 cm slit in the front side of the restrainer and the rest of their bodies were shielded behind a 5 cm-thick lead block (Fig. 1). The absorbed doses for the head and the body are shown in Fig. 2. For total body irradiation (to evaluate direct splenic damage following irradiation), the whole body was irradiated (up to 5 Gy).

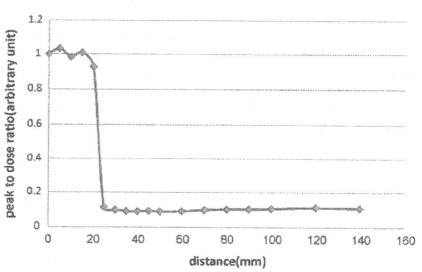

Fig. 2. Estimation of the amount of radiation passing through the 2 cm slit (the irradiated head dose) and into the area shielded by the lead block (the spleen dose). Each point corresponds to a red mark on the scale in Fig. 1. The intervals between the points were 5 mm (0–5 cm), 1 cm (5–10 cm) and 2 cm (10–14 cm). The head of the mouse was located in the first 2 cm (in the open region). The spleen was located at 4 cm. The dose given to the spleen was estimated at 1 Gy when 10 Gy of irradiation was given to the head.

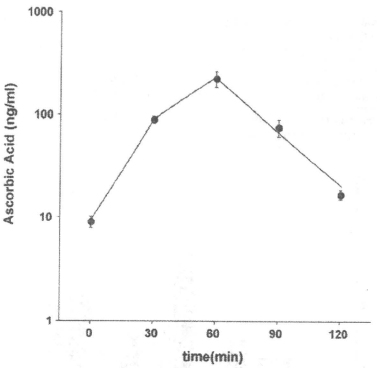

Fig. 3. The concentration of ascorbic acid in mouse plasma after AA-2G administration.

2.3. Isolation of splenocytes and splenic T lymphocytes

Details of the T lymphocyte isolation have been described elsewhere [15]. Briefly, after gamma irradiation, mice were sacrificed by cervical dislocation, and their spleens were removed, minced and washed twice in Hanks' balanced salt solution. Lymphocytes were separated using Ficoll-Hypaque gradients and were resuspended in RPMI 1640 medium (GIBCO) containing 10% fetal calf serum. The T lymphocytes were cultured at 37 °C in a humidified 5% CO_2 incubator. Optimum concentrations of Concanavalin A (Con A, 2 μg/mL) and 2-mercaptoethanol (2-ME, 50 μmol/mL) were used to make lymphocytes transform and divide in culture.

2.4. Radiation induced apoptosis and antioxidant enzyme activation

To determine splenocyte apoptosis, mice were sacrificed 24 h after irradiation and their spleens were removed. Single-cell suspensions were eliminated of erythrocytes by incubating at room temperature for 3 min in a solution of Tris-

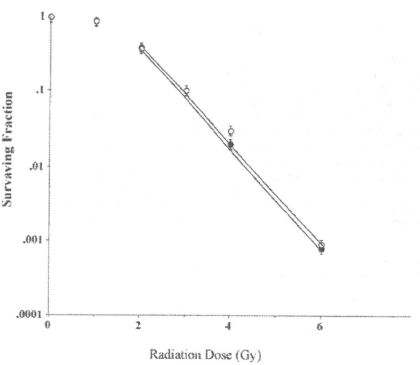

Fig. 4. Survival curves for splenic T lymphocytes following gamma irradiation with (open circle) or without (closed circle) ascorbic acid administration. Data represent the means ± SE of three different independent experiments. The curves for doses greater than 2 Gy were fit by linear regression analysis.

Table 1
Survival parameters for T lymphocytes after gamma ray irradiation with V.C. (ascorbic acid) treatment.

Treatment	D_0	D_{10}
Gamma ray radiation	0.65 ± 0.2 Gy	3.0 ± 0.2 Gy
Gamma ray radiation with V.C. treatment	0.85 ± 0.3 Gy	3.1 ± 0.2 Gy

Data pooled from three or more experiments; mean ± SE. D_0 and D_{10} derived from survival curves following irradiation.

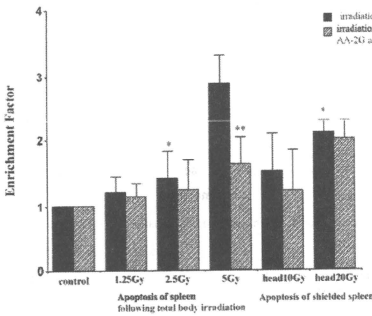

Fig. 5. Induction of apoptosis of mouse splenocytes after irradiation (black bars) and the effect of AA-2G administration (gray bars). Histogram bars show the means ± SE for five animals. (*) Significant increase in apoptosis compared to 2.5 Gy total body irradiation. $p < 0.05$. (**) Significant decrease in apoptosis compared to no ascorbic acid administration. $p < 0.05$.

buffered ammonium chloride. After twice washing with PBS, cells were counted and examined for induction of apoptosis. Apoptosis was detected with a sandwich immunoassay system using a cell death detection ELISA kit (Roche Diagnostic Inc.). The assay is based on the quantitative sandwich enzyme immunoassay principle, using mouse monoclonal antibodies directed against DNA and histones, respectively. Apoptosis was measured by following the ELISA protocol. The enrichment factor was the calculated absorbance of each sample divided by the absorbance of corresponding negative control. To measure the activity of catalase (CAT) and superoxide dismutase (SOD), mouse blood was obtained from the main inferior vein 60, 120 and 1200 min after irradiation. The activities of CAT and SOD in mouse plasma were detected using a colorimetric assay (SRL Research Laboratory Inc., Japan).

2.5. Determination of T lymphocyte survival and the micronucleus assay

Details of the assays for cell survival and micronucleus frequency have been reported previously [15]. Briefly, the survival data for lymphocytes were obtained by limiting dilution assays. To measure the cloning efficiency of lymphocytes, cells were seeded in culture medium (150 μL) at densities of 10–10,000 cells/well in 96-well tissue culture plates. The cloning efficiency was calculated from the proportion of the wells without clones, using limiting dilution analysis [16]. The cytokinesis-block micronucleus assay for lymphocytes was performed following a method described by Fenech and Morley [17] with slight modifications. Cytochalasin B (Sigma) was added to the cultured T lymphocytes at a final concentration of 5.0 μg/mL, 44 h after Con A stimulation. Eighteen hours later, cells were collected by centrifugation and resuspended in Carnoy's fixative. Next, a drop of the cell suspension was spread on a glass slide and dried, the cells were stained with Hoechst 33258 (50 μg/mL), and the frequency of micronuclei was determined on 10 separate slides by counting the total number of micronuclei per 100 binucleated cells.

Table 3
The micronucleus frequency per 100 binucleated T lymphocytes after irradiation and the effect of AA-2G administration.

Total body irradiation (Gy)			Head irradiation 10 Gy
0 Gy	1.25 Gy	2.5 Gy	
2.8 ± 1.5	26.8 ± 6.5	47.9 ± 13.2	62.1 ± 18.5
With AA-2G treatment			
2.9 ± 1.5	14.9 ± 8.5**	29.1 ± 11.5**	24.9 ± 10.5**

Results show the mean ± SE from at least three independent experiments.
** Significant differences were observed with AA-2G administration (Student's *t*-test; $p < 0.05$).

2.6. Statistical analysis

Significance was calculated using Student's tests. Results were considered significant for values of $p < 0.05$.

3. Results

3.1. The effect of ascorbic acid treatment

The ascorbic acid concentration in mouse plasma increased and was maintained at a high level during the 30–90 min after oral administration of AA-2G. One hour after AA-2G administration (1 mg/g of mouse body weight), the concentration of ascorbic acid in the plasma was increased 4–10× over the control (Fig. 3). The plasma level of ascorbic acid increased sharply, as quickly as 30 min, and was maintained at a high level for 1.5 h after oral administration of AA-2G. The availability of AA-2G as ascorbic acid was compatible with a previous report [13].

Fig. 4 and Table 1 show survival curves and the parameters for T lymphocytes after gamma irradiation, with and without ascorbic acid treatment. These results showed that gamma radiation lethality was not affected by ascorbic acid treatment.

3.2. Induction of apoptosis and the activities of anti-oxidative enzymes

Apoptosis was analyzed after 1.25, 2.5 and 5 Gy of whole body irradiation and 10 and 20 Gy of local head irradiation, with and without ascorbic administration. For local head irradiation, the spleen was shielded behind a 5 cm-thick lead block (Fig. 1) and the doses of radiation absorbed by the spleen and head were measured (1.0 Gy for the spleen from 10 Gy of radiation exposure to the head; 2.0 Gy (spleen) from 20 Gy (head); Fig. 2). After 20 Gy head irradiation, the apoptosis that occurred in shielded spleen cells exceeded that which occurred when spleen cells were directly irradiated with 2.5 Gy (Fig. 5). Therefore, the damage to shielded spleen cells was more excessive than what would be expected given a dose of 2.0 Gy.

Fig. 5 also shows the induction of apoptosis in mouse splenocytes after AA-2G treatment. Ascorbic acid protected mouse

Table 2
SOD and catalase activity in mouse serum after treatment with AA-2G.

Time after irradiation (min)	SOD activity (Units/mL)		Catalase activity (Units/mL)	
	6 Gy irradiation	6 Gy irradiation with AA-2G	6 Gy irradiation	6 Gy irradiation with AA-2G
0	7.7 ± 0.8	7.1 ± 0.7	1.0 ± 0.1	1.0 ± 0.1
60	9.2 ± 0.9	10.4 ± 1.0	3.6 ± 0.4	4.2 ± 0.4
120	10.0 ± 0.9	11.0 ± 1.0	3.6 ± 0.4	4.4 ± 0.4
1200	12.5 ± 1.0	14.0 ± 1.4	2.2 ± 0.2	4.4 ± 0.4**

Results show the mean ± SE from at least three independent experiments.
** Significant increases were observed with AA-2G administration (Student's *t*-test; $p < 0.05$).

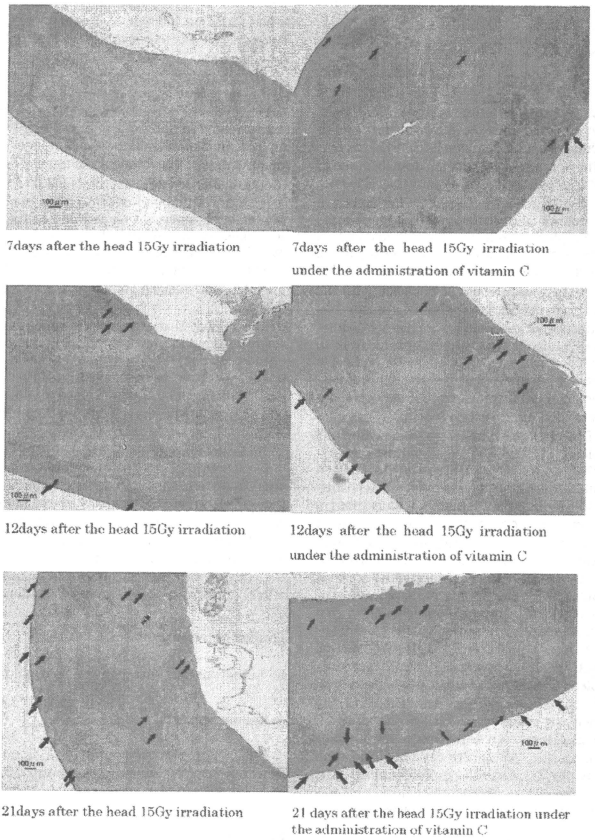

Fig. 6. Spleens 7–21 days after 15 Gy of head irradiation. Formalin-fixed paraffin-embedded tissue sections were HE stained. The arrows show macrophage proliferation in the spleen after the head irradiation (magnification 30×. Scale bars 100 μm).

splenocytes from apoptosis after 5 Gy whole-body irradiation. To understand how anti-oxidative enzymes participate in initial DNA damage, we investigated how treating with AA-2G affected the activation of the CAT and SOD in the plasma following a dose of 6 Gy (1 Gy in addition to the 5 Gy irradiation). AA-2G administration increased the activation of CAT and SOD slightly. A significant increase in CAT activity was observed with AA-2G treatment 20 h after irradiation (Table 2).

3.3. Micronucleus induction

The induction of micronuclei in mouse T lymphocytes after various treatments is shown in Table 3. Micronuclei were counted after 1.25 and 2.5 Gy of whole body irradiation and 10 Gy of local head irradiation, with and without ascorbic administration. As mentioned above, a 10 Gy dose of radiation exposure to the head corresponded to a dose of 1.0 Gy for the shielded spleen. The frequency of micronuclei induced in shielded splenic T cells with 10 Gy of head irradiation was about 2 times higher than that induced after 2.5 Gy of whole body irradiation (Table 3). Our results confirm that shielded, distant splenic T lymphocytes had more damage than what would have been anticipated, given a dose of 1.0 Gy. This again suggests that the radiation effects in a distant, shielded organ were enhanced after local irradiation. However, while treatment with ascorbic acid protected, although not significantly, against the induction of apoptosis in shielded splenocytes, ascorbic acid significantly inhibited shielded splenic T lymphocytes from forming micronuclei after local head irradiation (Fig. 5 and Table 3). Therefore, unlike its effects on induction of mouse splenocyte apoptosis, AA-2G had radioprotective

effects on the induction of T lymphocyte micronuclei after irradiation.

4. Discussion

In high LET therapy, as occurs in boron neutron capture therapy (BNCT) and heavy-ion radiotherapy, hypo-fractionation is acceptable and therapeutic radiation doses are larger than conventional radiotherapies. The normal tissue radiation dose for vascular endothelial cells in BNCT is estimated to be around 10–15 Gy [18]. Enhanced radiation effects in abscopal regions following large local doses of radiation have not previously been investigated. Here, we studied whether shielded splenocytes in abscopal regions suffered enhanced radiation effects after 10–20 Gy of local head gamma ray-irradiation. Splenocyte apoptosis induction and T lymphocyte micronuclei were higher than what would be expected with the estimated dose of radiation in the distant, shielded spleen.

In vivo radiation-induced bystander effects are defined as phenomena that occur when irradiation signals are transduced from an irradiated lesion to a shielded organ and induce a radiation effect in that non-irradiated, shielded organ. A previous group reported that the spleen is a target organ of local-irradiation induced bystander effects in vivo. Koturbash et al. described how cranial X-ray irradiation (1 Gy) induced DNA damage, apoptosis, and increased p53 levels in a shielded spleen [5]. They also suggested the possibility that the induction of indirect DNA damage in the shielded splenocytes was mediated by reactive oxygen species. Mechanistically, the radiation-induced bystander effect in vivo is thought to be mediated by the inflammatory response after exposure to ionizing radiation. Lorimore et al. reported that macrophage activation following a 4 Gy irradiation provided a mechanism for producing damage via bystander effects [19]. Another previous report showed that tumor cell killing by macrophages was activated with more than 10 Gy [20]. These experiments show that high dose radiation might induce bystander signaling by mediating macrophage activation. We confirmed that large dose local head irradiation (10–20 Gy) induced apoptosis and micronuclei in the distant, shielded spleen. These enhanced radiation effects in an abscopal region were induced by a large dose irradiation and may have been mediated by macrophage activation. Shown in the left column of Fig. 6, histological sections revealed macrophage proliferation in the spleen appearing on the 12th day post-irradiation and becoming severe by day 21. Macrophage proliferation in the spleen was found to be more severe after ascorbic acid administration, and to occur earlier (on the 7th day post-irradiation; shown in the right column of Fig. 6).

We evaluated the protective effects of a radical scavenger on enhanced radiation effects in the distant spleen after large doses of local head irradiation. Free radicals are one of the most important bio-chemicals that are triggered by the activation of macrophages following irradiation [21]. This suggests the possibility that radical scavengers might protect abscopal regions from enhanced radiation effects. Our study of apoptosis induction suggests that AA-2G treatment suppressed the induction of apoptosis following total body radiation. In our anti-oxidative enzyme study, AA-2G administration increased catalase activity after 20 h, which was the length of the apoptosis assay, but AA-2G did not significantly affect SOD activity. The C3H/He mouse strain is more radiation-resistant than other Balb/c mouse strains [22,23]. The different sensitivities of mouse strains to irradiation were determined by micronucleus formation in T lymphocytes and fibroblasts, and an intestinal cell survival assay [15]. A previous report demonstrated that hepatic CAT and SOD enzyme activities increased 30 min after whole body ionizing irradiation of C3H mice, suggesting that CAT and SOD may be related to the mechanism of their radiation resistance [24]. We confirmed that these antioxidant enzymes had elevated activities after irradiation and that AA-2G enhanced CAT activity. This result suggests that ascorbic acid may protect from radiation damage by inducing CAT.

We previously reported that radical scavengers are protective against neutron-induced mutations [25,26]. Furthermore, we compared the effects of DMSO (a source of short-lived radical scavengers) and ascorbic acid (a source of long-lived radical scavengers) on the induction of mutations in bystander cells. DMSO treatment slightly reduced the frequency of mutations that were induced by the bystander effect, but post-radiation ascorbic-acid treatment reduced the mutation frequency more than DMSO [10]. Recently, Harada et al. reported that ascorbic acid was an effective radical scavenger for suppressing the bystander response in vitro. They examined three types of radical scavengers, including a nitric oxide scavenger, and found that ascorbic acid was the most effective suppressor of micronucleus induction in non-irradiated bystander cells [27].

We showed that ascorbic acid significantly inhibited shielded splenic T lymphocytes from forming micronuclei following local head irradiation (Fig. 5 and Table 3). However, AA-2G did not protect shielded splenocytes against apoptosis. These results show that AA-2G treatment had radio-protective effects on T-lymphocytes in abscopal regions (in the spleen), but this did not apply to all splenic cells.

Clinically, chromosomal instability [28] and epigenetic dysregulation of DNA [29] were analyzed in non-irradiated or distant organs after irradiation. Enhanced radiation effects in abscopal regions are thought to increase the incidence of secondary, post-radiation therapy cancers. Therefore, effective radioprotection from enhanced radiation effects in abscopal regions is needed. Ascorbic acid is a well-known, important vitamin and a non-toxic radical scavenger that can be effective for protecting against enhanced radiation effects in abscopal regions during radiation therapy.

Conflict of interest

Authors declare that there are no conflicts of interest.

Acknowledgments

This study was supported by a Grant-in-Aid for Scientific Research from the Ministry of Education, Culture, Sports, Science and Technology of Japan.

References

[1] M.P. Nobler, The abscopal effect in malignant lymphoma and its relationship to lymphocyte circulation, Radiology 93 (1969) 410–412.
[2] W.F. Morgan, Non-targeted and delayed effects of exposure to ionizing radiation: II. Radiation-induced genomic instability and bystander effects in vivo, clastogenic factors and transgenerational effects, Radiat. Res. 159 (2003) 581–596.
[3] K. Camphausen, M.A. Moses, C. Menard, M. Sproull, W.D. Beecken, J. Folkman, M.S. O'Reilly, Radiation abscopal antitumor effect is mediated through p53, Cancer Res. 63 (2003) 1990–1993.
[4] E.I. Azzam, J.B. Little, The radiation-induced bystander effect: evidence and significance, Hum. Exp. Toxicol. 23 (2004) 61–65.
[5] I. Koturbash, J. Loree, K. Kutanzi, C. Koganow, I. Pogribny, O. Kovalchuk, In vivo bystander effect: cranial X-irradiation leads to elevated DNA damage, altered cellular proliferation and apoptosis, and increased p53 levels in shielded spleen, Int. J. Radiat. Oncol. Biol. Phys. 70 (2007) 554–562.
[6] K.M. Prise, M. Folkard, B.D. Michael, A review of the bystander effect and its implications for low-dose exposure, Radiat. Protect. Dosimetry 104 (2003) 347–355.
[7] G.W. Morgan, S.N. Breit, Radiation and the lung: a re-evaluation of the mechanism mediating pulmonary injury, Int. J. Radiat. Oncol. Biol. Phys. 31 (1995) 361–369.
[8] M.A. Khan, R.P. Hill, J. Van Dyk, Partial volume rat lung irradiation: an evaluation of early DNA damage, Int. J. Radiat. Oncol. Biol. Phys. 40 (1998) 467–476.

[9] K.M. Prise, M. Folkard, B.D. Michael, Bystander response induced by low LET radiation, Oncogene 22 (2003) 7043–7049.
[10] Y. Kinashi, S. Masunaga, K. Nagata, M. Suzuki, S. Takahashi, K. Ono, A bystander effect observed in boron neutron capture therapy: a study of the induction of mutations in the HPRT locus, Int. J. Radiat. Oncol. Biol. Phys. 68 (2007) 508–514.
[11] G. Kashino, K.M. Prise, K. Suzuki, N. Matsuda, S. Kodama, M. Suzuki, K. Nagata, Y. Kinashi, S. Masunaga, K. Ono, M. Watanabe, Effective suppression of bystander effects by DMSO treatment of irradiated CHO cells, J. Radiat. Res. 48 (2007) 197–204.
[12] I. Yamamoto, S. Suga, Y. Mitoh, M. Tanaka, N. Muto, Antiscorbutic activity of L-ascorbic acid 2-gluciside and its availability as a vitamin C supplement in normal rats and guinea pigs, J. Pharmacobiodyn. 13 (1990) 688–695.
[13] A. Tai, Y. Fujitani, K. Matsumoto, D. Kawasaki, I. Yamamoto, Bioability of a series of novel acylated ascorbic acid derivatives, 6-O-acyl-2-O-α-D-glucopyranosyl-L-ascorbic acids, as an ascorbic acid supplement in rats and guinea pigs, Biosci. Biotechnol. Biochem. 66 (2002) 1628–1634.
[14] L.V. d'Uscio, S. Milstien, D. Richardson, L. Smith, Z.S. Katusic, Long-term Vitamin C treatment increase vascular tetrahydrobiopterin levels and nitric oxide synthase activity, Circulat. Res. 92 (2003) 88–95.
[15] Y. Kinashi, K. Ono, M. Abe, The micronucleus assay of lymphocytes is a useful predictive assay of the radiosensitivity of normal tissue: a study of three inbred strains of mice, Radiat. Res. 148 (1997) 341–347.
[16] H. Waldmann, S. Cobbold, I. Lefkovits, Limiting dilution analysis, in: G.G.B. Klaus (Ed.), Lymphocytes, A Practical Approach, IRL, Oxford, 1987, pp. 163–188.
[17] F. Fenech, A.A. Morley, Cytokinesis-block micronucleus method in human lymphocytes: effect of in vivo aging and low dose X-irradiation, Mutat. Res. 161 (1986) 193–198.
[18] T. Kageji, S. Nagahiro, S. Uyama, Y. Mizobuchi, Y. Nakagawa, Clinical review of BNCT using mixed neutron beam in patients with malignant glioma, in: W. Sauerwein, R. Moss, A. Wittig (Eds.), Research and Development in Neutron Capture Therapy Monduzzi Editore S.p.A., Bologna, Italy, 2002, pp. 1085–1091.
[19] S.A. Lorimore, P.J. Coates, G.E. Scobie, G. Milne, E.G. Wright, Inflammatory-type responses after exposure to ionizing radiation in vivo: a mechanism for radiation-induced bystander effects? Oncogene 20 (2001) 7085–7095.
[20] L.E. Lambert, D.M. Paulnock, Modulation of macrophage function by γ-irradiation; Acquisition of the primed cell intermediate stage of macrophage tumoricidal action pathway, J. Immunol. 139 (1987) 2834–2841.
[21] G. McLennan, L.W. Oberley, A.P. Author, The role of oxygen-derived free radicals in radiation-induced damage and death of nondividing eukaryotic cells, Radiat. Res. 84 (1980) 122–132.
[22] K.H. Kohn, M.M. Kallman, The influence of strain on acute X-ray lethality in the mouse: LD50 and death rate studies, Radiat. Res. 5 (1956) 309–317.
[23] T.H. Roderic, The response of twenty-seven inbred strains of mice to daily doses of whole-body X-irradiation, Radiat. Res. 120 (1963) 631–639.
[24] R. Hardmeier, H. Hoeger, S. Fang-Kircher, A. Khoschsorur, G. Lubic, Transcription and activity of antioxidant enzymes after ionizing irradiation in radiation-resistant and radiation-sensitive mice, Proc. Natl. Acad. Sci. U.S.A. 94 (1997) 7572–7576.
[25] Y. Kinashi, Y. Sakurai, S. Masunaga, M. Suzuki, M. Akaboshi, K. Ono, Dimethyl sulfoxide protects against thermal and epithermal neutron-induced cell death and mutagenesis of Chinese hamster ovary (CHO) cells, Int. J. Radiat. Oncol. Biol. Phys. 47 (2000) 1371–1378.
[26] Y. Kinashi, Y. Sakurai, S. Masunaga, M. Suzuki, K. Nagata, K. Ono, Ascorbic acid reduced mutagenicity at the HPRT locus in CHO cells against thermal neutron radiation, Appl. Radiat. Isotopes 61 (2004) 929–932.
[27] T. Harada, G. Kashino, K. Suzuki, N. Matsuda, S. Kodama, M. Watanabe, Different involvement of radical species in irradiated and bystander cells, Int. J. Radiat. Biol. 84 (2008) 809–814.
[28] E. Gwyneth, S.A. Watson, A. Lorimore, D.A. Macdonald, E.G. Wright, Chromosomal instability in unirradiated cells induced in vivo by a bystander effect of ionizing radiation, Cancer Res. 60 (2000) 5608–5611.
[29] I. Koturbash, A. Boyko, R. Rodriguez-Juarez, R.J. MacDonald, V.P. Tryndyak, I. Kovalchuk, I.P. Pogribny, O. Kovalchuk, Role of epigenetic effects in maintenance of long-term persistent bystander effect in spleen in vivo, Carcinogenesis 28 (2007) 1831–1838.

Advanced Drug Delivery Reviews 63 (2011) 161–169

Contents lists available at ScienceDirect

Advanced Drug Delivery Reviews

journal homepage: www.elsevier.com/locate/addr

Intracellular targeting delivery of liposomal drugs to solid tumors based on EPR effects ☆

Kazuo Maruyama *

Faculty of Pharmaceutical Sciences, Teikyo University, 1091-1, Suarashi, Midori-ku, Sagamihara, 252-5195 Japan

ARTICLE INFO

Article history:
Received 18 March 2010
Accepted 1 September 2010
Available online 28 October 2010

Keywords:
Liposome
PEG-liposome
Transferrin
Boron neutron-capture therapy (BNCT)
Oxaliplatin
Passive targeting
Intracellular targeting
Fab' fragment

ABSTRACT

The success of an effective drug delivery system using liposomes for solid tumor targeting based on EPR effects is highly dependent on both size ranging from 100-200 nm in diameter and prolonged circulation half-life in the blood. A major development was the synthesis of PEG-liposomes with a prolonged circulation time in the blood. Active targeting of immunoliposomes to the solid tumor tissue can be achieved by the Fab' fragment which is better than whole IgG in terms of designing PEG-immunoliposomes with prolonged circulation. For intracellular targeting delivery to solid tumors based on EPR effects, transferrin-PEG-liposomes can stay in blood circulation for a long time and extravasate into the extravascular of tumor tissue by the EPR effect as PEG-liposomes. The extravasated transferrin-PEG-liposomes can maintain anti cancer drugs in interstitial space for a longer period, and deliver them into the cytoplasm of tumor cells via transferrin receptor-mediated endocytosis. Transferrin-PEG-liposomes improve the safety and efficacy of anti cancer drug by both passive targeting by prolonged circulation and active targeting by transferrin.

Contents

1. Introduction

It was the German bacteriologist Paul Ehrlich who, in the late nineteenth century, coined the term "magic bullet", meaning a chemical that travels through the body and selectively kills diseased cells without harming neighboring healthy cells. Since then, many different approaches based on various physical and biochemical principles have been examined with the goal of developing systems with a therapeutically acceptable degree of target specificity. Understanding target structure and function, developing drug delivery strategies to achieve controlled release, and targeting of drugs to specific tissues of the body, have been a major focus of research in an attempt to improve selectivity in cancer treatment. Currently, the concept of the "magic bullet" includes a coordinated behavior of three components: (A) drug; (B) targeting moiety; and (C) pharmaceutical carrier. Pharmaceutical carriers include soluble polymers, microcapsules, microparticles, cells, cell ghosts, proteins including monoclonal antibody, lipoproteins, micelles, and liposomes.

The use of liposomes in drug delivery as the "magic bullet" has been extensively studied (for recent books, see ref. [1,2]). Liposomal carriers have a strong impact on pharmacokinetics and on the tissue distribution of incorporated drugs. The pharmacokinetic parameters

☆ This review is part of the *Advanced Drug Delivery Reviews* theme issue on "EPR effect based drug design and clinical outlook for enhanced cancer chemotherapy".

* Corresponding author. Tel.: +81 42 685 3722; fax: +81 42 685 3432.
E-mail address: maruyama@pharm.teikyo-u.ac.jp.

0169-409X/$ – see front matter © 2010 Elsevier B.V. All rights reserved.
doi:10.1016/j.addr.2010.09.003

of liposomes depend on the physicochemical characteristics of the liposomes, such as size, surface charge, membrane lipid packing, steric stabilization, dose, and route of administration [3,4]. These factors may lead to enhanced efficacy as well as reduced toxic side effects of antitumor drugs. Clinical trials have demonstrated a reduced risk of cardiotoxicity of normal and pegylated liposomal doxorubicin including compared to the free drug, while preserving antitumor activity [5]. However, a major drawback of liposomes is their rapid uptake and accumulation by phagocytic cells of the mononuclear phagocyte system (reticuloendothelial system (RES)) after systemic administration [6]. Conventional liposomes are opsonized by plasma proteins, quickly recognized as foreign bodies, and rapidly captured by the RES. The major organs of accumulation are the liver and the spleen due to their rich blood supply and the abundance of tissue-resident phagocytic cells. Such unwanted macrophage uptake during chemotherapy can be problematic since it may lead to partial depletion of macrophages and interfere with important host-defense functions of this cell type [7]. Depending on the size and composition of the liposome, RES uptake can occur within minutes after administration and remove the liposomes from the circulation. A liposome with a diameter larger than 400 nm cannot circulate in the blood stream for long since it is quickly captured by the RES, whereas a liposome with a diameter<200 nm can remain in circulation for a long time [8,9].

The blood vessels in most normal tissues are non-fenestrated capillaries. These blood vessels are composed of a single layer of endothelial cells with tight junctions. In contrast, tumor blood vessels are inherently leaky, due to wide inter-endothelial junctions, the large number of fenestrae and transendothelial channels formed by vesicles, and a discontinuous or absent basement membrane [10,11]. Generally, the capillary permeability of the endothelial barrier in newly vascularized tumors is significantly greater than that of normal tissues [12].

The extravasation of liposomes from blood vessels to the tumor region is a function of both local blood flow and microvascular permeability [12]. Liposomes of the appropriate size can accumulate relatively easily into well-vascularized tumors through vascular fenestrations. However, it may take a long time for the liposome to reach an effective or maximum drug concentration level in the tumor or target site. In addition, due to little or no lymphatic drainage in tumor tissues, liposomes are, upon accumulation, retained in the tumor interstitium for a prolonged period. This phenomenon, termed the enhanced permeability and retention (EPR) effect, has been shown to occur universally among tumor types [13,14]. Therefore, the success of an effective drug delivery system using liposomes for tumor targeting based on EPR effects is highly dependent on prolonged circulation in the blood.

2. Passive targeting of the liposomal carrier to solid tumors based on EPR effects

To reach a target solid tumor site, liposomes must find the fenestrate (opening) on the tumor blood vessels through conventional flow and random diffusional processes. These processes, which are linked to probability issues, are called "passive targeting" coupled with "enhanced permeability". A major development in the last decade of the twentieth century was the synthesis of PEGylated liposomes (PEG-liposomes) with a prolonged circulation time in the blood. These liposomes are commonly called "stealth" liposomes, long-circulating liposomes, or sterically stabilized liposomes. PEG-liposomes containing polyethylene glycol derivatives of phosphatidyl ethanolamine (PEG-lipid) are not readily taken up by macrophages in the RES, and hence remain in the circulation for a relatively long period [15–18]. Normally, plasma proteins are easily adsorbed onto conventional liposome surfaces, easily caught by the RES, and eliminated from the body [9,19]. To avoid this rapid clearance, a hydrophilic compound is coated on the surface of the liposomes [15,20,21]. When PEG-lipid is inserted into liposomal membranes, an aqueous layer is formed by the localization of the PEG tether on the surface and adheres to the liposomes [22]. This modification prevents the recognition of the liposomes by opsonins (i.e., antibodies or components of the complement system) and therefore reduces their clearance by cells of the RES [23]. PEG-liposomes can remain in the blood circulation for extended periods (i.e., $t_{1/2}$>40 h) and distribute through an organism relatively evenly. Most of the liposomes distribute in the central compartment (i.e., the blood), with only 10% to 15% of the dose being delivered to the liver. This is a significant improvement over conventional liposomes where typically 80% to 90% of the liposomes deposit in the liver.

The extravasation of different-sized PEG-liposomes into solid tumors was examined in various tumor models in mice [24 and unpublished data]. As shown in Fig. 1 (left), long-circulating liposomes composed of DSPC/Chol/DSPE-PEG2000 (1:1:0.13, m/m) with an average diameter of 100-200 nm were accumulated efficiently in all tumor tissues examined. Liposome size was clearly another important factor for extravasation. Observations using fluorescence microscopy have shown that PEG-liposomes can indeed extravasate beyond the endothelial barrier mainly in postcapillary venules [25,26]. Extravasation and localization of PEG-liposomes were also examined by electron microscopy in Colon 26 tumor-bearing mice. As shown in Fig. 1 (right), wide inter-endothelial junctions were observed in tumor sections containing blood vessels. PEG-liposomes escaped from the gaps between adjacent endothelial cells and extensively penetrated into the extravascular and interstitial space among tumor cells. The size of the gaps between the cells that line tumor blood vessels has been estimated to be 100-600 nm [27], that is sufficiently large to allow the extravasation of small PEG-liposomes from the vessel to tumor interstitial space. Due to the increased circulation time of liposomes containing PEG-lipid and the leaky structure of microvasculature in the solid tumor tissue, these liposomes have been shown to accumulate preferentially in tumor tissue. Thus, under physiological tumor conditions, only small liposomes ranging from 100-200 nm in diameter with a prolonged circulation half-life have a significant chance of encountering the leaky vessels of tumor tissue.

3. Clinical development of liposomal anti-cancer drugs based on EPR effects

Base on the EPR effect, many liposomal drugs for passive targeting are being developed as a new class of antitumor agents [28–30]. At present, several liposomal anticancer drugs are available in the clinic or are in advanced stages of clinical development, as shown in Table 1. Clinical studies have shown that conventional liposomes are taken up by liver macrophages and destroyed with a half-life in body fluids of 20 min [31]. On the contrary, PEG-liposomes display a half-life of 5 days in these body fluids [32]. Liposomal drug formulations offer the possibility of increasing efficacy while reducing the toxic side effects of cytotoxic chemotherapeutic drugs.

The clinical use of liposomal formulations of conventional cytostatic drugs focused initially on anthracyclines, since these cationic amphiphiles allow efficient and stable liposomal entrapment. Liposomal formulations of anthracyclines are used for the treatment of ovarian and breast cancer, and of HIV associated Kaposi's sarcoma. Anthracyclines bear a high risk of causing acute and cumulative cardiotoxicity (resulting in cardiomyopathy), which limits their use. Liposomal formulations can solve these problems [28,33] since the altered pharmacokinetics of liposomal anthracyclines offers the possibility of avoiding high plasma peaks owing to drug retention within the liposomal formulation.

There are very interesting summarized data by Huwyler et al. [34] that compare the pharmacokinetic properties in human of Doxil/